NIH Public Access
Author Manuscript
Eur J Neurosci. Author manuscript; available in PMC 2010 September 1.

Published in final edited form as:
Eur J Neurosci. 2009 September ; 30(6): 1036–1055. doi:10.1111/j.1460-9568.2009.06896.x.

Lack of kainic acid-induced gamma oscillations predicts subsequent CA1 excitotoxic cell death

Seiichiro Jinde[1,*], **Juan E. Belforte**[1,**], **Jun Yamamoto**[2], **Matthew A. Wilson**[2], **Susumu Tonegawa**[2,3], and **Kazu Nakazawa**[1]

[1] Unit on Genetics of Cognition and Behavior, Mood and Anxiety Disorders Program, National Institute of Mental Health, National Institutes of Health, Department of Health and Human Services, Maryland 20892

[2] The Picower Institute for Learning and Memory, RIKEN-MIT Center for Neural Circuit Genetics, Massachusetts Institute of Technology, Cambridge, Massachusetts 02139

[3] Howard Hughes Medical Institute.

Abstract

Gamma oscillations are a prominent feature of hippocampal network activity, but their functional role remains debated, ranging from mere epiphenomenon to crucial for information processing. Similarly, persistent gamma oscillations sometimes appear prior to epileptic discharges in patients with mesial temporal sclerosis. However, the significance of this activity in hippocampal excitotoxicity is unclear. We assessed the relationship between kainic acid (KA)-induced gamma oscillations and excitotoxicity in genetically-engineered mice in which *N*-methyl-D-aspartic acid (NMDA) receptor deletion was confined to CA3 pyramidal cells. Mutants showed reduced CA3 pyramidal cell firing and augmented sharp wave-ripple activity, resulting in higher susceptibility to KA-induced seizures, and leading to strikingly selective neurodegeneration in the CA1 subfield. Interestingly, the KA-induced gamma-aminobutyric acid (GABA) level increases and persistent 30-50 Hz gamma oscillations observed in control mice prior to the first seizure discharge was abolished in the mutants. Consequently, on subsequent days, mutants manifested prolonged epileptiform activity and massive neurodegeneration of CA1 cells, including local GABAergic neurons. Remarkably, pretreatment with the potassium channel blocker α-dendrotoxin (DTX) increased GABA levels, restored gamma oscillations, and prevented CA1 degeneration in the mutants. These results demonstrate that emergence of low frequency gamma oscillations predicts increased resistance to KA-induced excitotoxicity, raising the possibility that gamma oscillations may have potential prognostic value for the treatment of epilepsy.

Keywords

CA3; NMDA receptors; GABA; Epilepsy Research; mouse

Correspondence should be addressed to: Kazu Nakazawa, M.D., Ph.D. Unit on the Genetics of Cognition and Behavior Mood and Anxiety Disorders Program National Institute of Mental Health Building 35, Room 1C-915 Phone: (301) 451-3499 Fax: (301) 480-0123 nakazawk@mail.nih.gov .

[*] *Present address*: Department of Neuropsychiatry, Graduate School of Medicine, The Unversity of Tokyo, 7-3-1 Hongo, Bunkyo-ku, Tokyo 113-8655, Japan.

[**] *Present address*: Department of Physiology, School of Medicine, University of Buenos Aires, Paraguay 2155 7 floor (1121), Buenos Aires, Argentina.

NIH-PA Author Manuscript
NIH-PA Author Manuscript
NIH-PA Author Manuscript

NIH-PA Author Manuscript

NIH-PA Author Manuscript

NIH-PA Author Manuscript

Introduction

Gamma oscillations in cortical structures, defined as synchronous rhythmic oscillatory activity from 30 to 100 Hz, are believed to play a role in neural communication and information processing (Singer & Gray, 1995; Buzsáki & Draguhn, 2004). While these physiological gamma oscillations are transiently induced by sensory stimulations (for hundreds of ms to 1 sec), persistent gamma oscillations lasting many sec or even min (Traub *et al*., 1999) have also been observed in human epileptic patients (Uhlhaas & Singer, 2006; Hughes, 2008); indeed, these gamma oscillations are often observed before or coincident with the onset of seizure discharges (Allen *et al*., 1992; Fisher *et al*., 1992; Alarcon *et al*., 1995; Medvedev, 2001; Jirsch *et al*., 2006). An increase in high-frequency (60-100 Hz) oscillations prior to the onset of neocortical seizures sometimes anticipates subsequent epileptic seizures (Worrell *et al*., 2004). In contrast, low gamma oscillations are typically associated with a favorable prognosis after resective surgery (Lee *et al*., 2000; Park *et al*., 2002). Therefore, their significance in excitotoxic insults has remained elusive.

Systemic and intrahippocampal injection of kainic acid (KA) in rodents induces epileptiform-like seizures and massive neurodegeneration, which has been used as an animal model of temporal lobe epilepsy (Schwob *et al*., 1980; Nadler, 1981; Ben-Ari, 1985; Sperk, 1994). Interestingly, KA administration also induces complex epileptiform EEG patterns, including gamma oscillations, which precede the ictal-like seizure discharges and generalized behavioral seizures (Bragin *et al*., 1999; Medvedev *et al*., 2000; Khazipov & Holmes, 2003; Sakatani *et al*., 2008). KA-induced oscillations in the CA3 subfield of the hippocampus are completely blocked by bicuculline, a γ-aminobutyric acid $(GABA)_A$ receptor antagonist, but they are largely maintained in the presence of the α-amino-3-hydroxy-5-methyl-4-isoxazolepropionic acid (AMPA) receptor antagonists in slice preparations (Fisahn *et al*., 2004), as well as *in vivo* preparations (Khazipov & Holmes, 2003). The strong reliance of gamma oscillations on $GABA_A$ receptors suggests these oscillations arise from a network of mutually connected GABAergic neurons (Whittington *et al*., 1995; Bartos *et al*., 2007; Mann & Paulsen, 2007). KA administration also produces neuronal degeneration, mainly in the limbic area of the brain, where hippocampal pyramidal cells are highly vulnerable (Schwob *et al*., 1980; Sperk, 1994). However, the relationship between the gamma oscillations that precede seizures and KA-induced excitotoxicity has, to date, not been explored.

In the current study, we initially assessed KA-induced seizure susceptibility in mice where NR1, the essential subunit of *N*-methyl-D-aspartic acid (NMDA) receptors, was selectively ablated from CA3 pyramidal cells [CA3-NR1 knockout (KO) mice, hereafter referred to as mutants] (Nakazawa *et al*., 2002). We found that compared to control mice, the mutants were more susceptible to KA-induced seizures and massive neurodegeneration that was confined to area CA1 of the hippocampus. Interestingly, in mutants, persistent 30-50 Hz gamma oscillations prior to seizure discharges were not detectable in area CA1. The relationship between the gamma oscillations that precede seizures and KA-induced excitotoxicity is discussed.

Materials and Methods

All experimental procedures were carried out in accordance with the National Research Council (NRC)'s Guide for the Care and Use of Laboratory Animals, and were approved by the National Institute of Mental Health (NIMH) Animal Care and Use Committee.

NIH-PA Author Manuscript

NIH-PA Author Manuscript

NIH-PA Author Manuscript

Animals

Subjects were naïve males of CA3-NR1 KO (Cre +/−; NR1 flox/flox) mutant mice and their three control littermates; floxed-NR1 (fNR1; Cre −/−; NR1 flox/flox), hemizygous G32-4(CA3)-Cre (Cre +/−; NR1 +/+), and wild-type mice from a C57BL/6NTac (B6) background. All mice were between the ages of 18 to 26 wk and were obtained by the same breeding method as previously described (Nakazawa *et al*., 2002). Two to 5 mice were housed per cage in a 12-h light/dark cycle, with access to food and water *ad libitum*. All the experiments were conducted by operators who were blind to the mouse genotypes. All efforts were made to minimize the number of animals used and their suffering. All animals undergoing seizures or that received the survival surgery for implantation of a microdrive or microwire array were monitored daily for signs of poor health, and any animal that developed moribund poor health was euthanized.

Behavioral seizure scoring

KA obtained from Sigma-Aldrich (St. Louis, MO, USA) or Tocris Bioscience (Ellisville, MO, USA) was dissolved in 0.9% saline at 5 mg/mL to keep the injection volume below 0.5 ml and was prepared fresh on the day of each experiment. To establish the optimal dose of KA that induced bilateral forelimb clonus and rearing in around 50% of animals, control fNR1 mice were given intraperitoneal (i.p.) injections of KA, at doses ranging from 15 to 30 mg/kg body weight. Behavioral seizure activity was monitored for 2 h by video camera and classified according to a modified Racine's scale (Racine, 1972): stage 0, normal behavior; stage 1, immobility; stage 2, repetitive movements, myoclonic twitch, or head bobbing; stage 3, bilateral forelimb clonus and rearing; stage 4, continuous rearing and falling; stage 5, generalized tonic-clonic seizure. Based on the result in Fig. S1, a dose of 20 mg/kg was established to elicit 'stage 3′ seizures in about 40% of fNR1 control mice with no mortality, and was used throughout the remainder of the experiments. Because no significant score differences were observed when using KA obtained from Sigma-Aldrich or Tocris Bioscience, the data obtained from each drug were combined for this study.

The mutant mice and their three strains of control littermates—fNR1, G32-4 Cre and B6—were given i.p. injections of 20 mg/kg KA, and the maximal seizure score was scored every 5 min over the entire 2-h observation period per animal. To evaluate the seizure susceptibility, the latency to 'stage 3′ seizure was measured. If the animal did not show a stage 3 seizure, 120 min was taken as the maximum latency. Occurrence (%) of 'stage 4′ seizure score as well as a cumulative seizure score for each animal during the 2-h period were averaged to calculate the rating scale value (± SEM) for each genotype. In order to evaluate the effect of α-dendrotoxin (DTX), a potent enhancer of presynaptic GABA release, on KA-induced seizures and subsequent events in the mutants, additional experiments were conducted. For instance, we tested various doses of DTX to determine the optimal subconvulsive dose of DTX. An i.p. injection of 0.5 mg/kg body weight induced subconvulsive seizures such as grooming, head nodding and occasional wet-dog shaking, but no convulsive seizure. Therefore, 0.5 mg/kg was chosen for the subsequent experiments. All the drugs, except KA from Tocris Bioscience, were purchased from Sigma-Aldrich.

Histological procedures

Mice were deeply anesthetized with Avertin (i.p. injection of 0.03ml of 2.5% tribromo-ethanol in tert-Amy alcohol per gram of body weight), and perfused transcardially with 4% paraformaldehyde 1 day, 7 days, and 4 wk after the KA treatment. Untreated animals were used as controls for each genotype. Brains were post-fixed in 4% paraformaldehyde overnight, and 40 μm-thick Vibratome sections were prepared for the following experiments. Our preliminary study showed no significant difference in histological features

NIH-PA Author Manuscript

NIH-PA Author Manuscript

NIH-PA Author Manuscript

among the three control genotypes. Therefore, fNR1 mice were chosen as controls for all the subsequent histological studies. In total, 30 fNR1 mice and 29 mutants were used.

To assess neuronal cellular degeneration, sections were stained with 0.2% Safranin O solution (Polyscience, Inc. Warrington, PA, USA) for Nissl staining. Fluoro-Jade B (Schmued & Hopkins, 2000) and neurosilver staining were used to demonstrate perikaryal and terminal degeneration. Fluoro-Jade B staining was performed according to the manufacturer's instruction (Histo-Chem, Inc., Jefferson, AR, USA). Briefly, sections were initially mounted, rehydrated with 80% ethanol and 70% ethanol, washed with distilled water, and incubated in 0.06% potassium permanganate solution for 10 min. The sections were then incubated in 0.0004% Fluoro-Jade B solution containing 0.1% glacial acetic acid for 15 min at room temperature, washed, and mounted with distrene plasticizer xylene (DPX; Electron Microscopy Sciences, Hatfield, PA, USA). For silver staining, free-floating 40-μm sections were processed with a silver impregnation protocol according to the manufacturer's instruction (NeuroSilver; FD Neurotechnologies Inc, Baltimore, MD, USA). To evaluate the relationship between behavioral seizure score and excitotoxic injury, the extent of the injury in the CA1 area was scored on a scale of 0-3, modified from the grading system (Pulsinelli *et al*., 1982) as a 'damage score' using Nissl staining as follows; score 0, no injury; score 1, 1-33%; score 2, 34-66%, score 3, 67-100% damage of CA1 cell layer.

Immunohistochemistry

To evaluate the functional integrity of hippocampal GABAergic neurons, 40 μm-thick parasagittal Vibratome sections were washed with PBS and blocked with 5% normal goat serum in PBS, followed by incubation at 4°C with gentle shaking in anti-glutamic acid decarboxylase (GAD)-67 mAb (1:5000, Millipore, Billerica, MA, USA) for three nights. Four sections per animal, which displayed 'stage 4′ or more severe behavioral seizures, were then incubated with Alexa488-conjugated anti-rat or mouse IgG (1:200, Molecular Probes, Eugene, OR, USA) at room temperature for 2 h. The number of GAD67-positive cells in CA1, CA3, and dentate gyrus (DG) was counted for each section, and the number of positive cells in area CA1 was further counted for each stratum (stratum oriens, pyramidale, radiatum or lacunosum-moleculare). The cell number was evaluated as a cell density, for which the cell number was divided by the area of each subregion/stratum, and was averaged per mouse. For double staining with anti-GAD67 and Fluoro-Jade B, sections after GAD67-immunostaining were washed in three changes of PBS (10 min each) and placed on silane-coated slide glasses, followed by a brief 1-min rinse in distilled water. The sections were then stained with 0.00001% Fluoro-jade B in 0.1% acetic acid for 20 min at room temperature, and washed in three changes of distilled water (for 1 min per wash) (Simpson *et al*., 2001).

To assess GABA levels during KA-induced gamma oscillations, the animals (8 mutants and 8 controls) were sacrificed 20 min after a KA administration (20 mg/kg i.p.). Seven mutants were treated with KA 90 min after pre-treatment with DTX (0.5 mg/kg i.p.), and then sacrificed 20 min after KA injection. Twenty-μm thick parasagittal cryostat sections from fresh-frozen brains were mounted on slides, followed by fixation with an ice-cold PBS solution containing 2% paraformaldehyde/2.5% glutaraldehyde for 10 min. GABA was labeled with anti-GABA primary antibody (1:1000, Millipore) and Alexa488-conjugated anti-mouse secondary antibody (1:200, Molecular Probes, Eugene, OR, USA), and the intensity of GABA-IR in the hippocampus was analyzed. To decrease variability in staining across animals, samples from different animals were immunostained together. To avoid any sampling bias that could affect GABA-IR quantification, two different parasagittal sections from around 1.9 μm and 2.3 μm from bregma were selected per mouse. Staining images were acquired and converted to grey scale, and analyzed with ImageJ software (NIH, Bethesda, MD, USA). The intensity of GABA-immunoreactivity (IR) was measured as a

NIH-PA Author Manuscript

NIH-PA Author Manuscript

NIH-PA Author Manuscript

mean grey value in the stratum pyramidale in CA1, the stratum lucidum in CA3, and corpus callosum per section. The grey value of CA1 and CA3 was normalized by the value of corpus callosum on the same section, and averaged per mouse.

In vivo multi-tetrode recording from area CA3

Naïve mice were implanted with a microdrive array consisting of seven independently adjustable tetrodes, six of which were targeted to CA3 (stereotaxic coordinates from bregma: 1.8 mm lateral; 2.0 mm posterior) and one to the corpus callosum to serve as the reference. The mouse microdrive array for the tetrode recording was originally designed by Dr. Linus D. Sun and was custom-made (Accelerated Technologies, Inc., Austin, TX, USA) with some modifications. It was directly connected to an EIB-27-Micro (Neuralynx, Bozeman, MT, USA), and unit recording was conducted using 32 channels of a Cheetah-64 recording system (Neuralynx). After 10 days of recovery from the implantation surgery, the tetrodes were slowly lowered into the CA3 as the mice were sitting quietly in a small high-walled enclosure (sleep box). Recordings began once stable units were obtained. Recording sessions generally consisted of one or two “Run” epochs (20-30 min each) bracketed by “sleep” sessions in which the animal rested quietly on a small platform outside of the behavioral environment. “Run” sessions were conducted in a low walled L-shaped linear track (length 77 cm and width 7 cm) placed near the center of a square black-curtained room (10 ft × 10 ft). Diffuse room lighting was provided by low intensity spotlights focused on four salient visual cues located on each of the walls of the recording room. Extracellular action potentials during an animal’s run were recorded while the animal’s position was tracked using a pair of infrared diodes placed 2 cm above its head. All the data acquired during recording sessions were analyzed offline. In order to analyze individual cells in X-clust, a manual clustering program (Wilson & McNaughton, 1993), Neuralynx timestamp tracking files and Neuralynx video tracking files were converted to the files on a linux template with the use of a custom interactive program running on a PC workstation. Action potentials were assigned to individual cells based on a spike’s relative amplitude across the four recording wires of a tetrode (Nakazawa *et al*., 2002). In order to be included for analysis, isolated cells had to satisfy three criteria: (i) fire a minimum of 100 spikes during the “Run” session, (ii) have a mean firing rate greater than 0.1 Hz, and (iii) have less than 0.5% of the cell spikes fall within a 1 ms refractory period. All isolated cells were divided into two subclasses—pyramidal cells and interneurons—based on waveform and firing characteristics. Putative pyramidal cells were defined as cells with relatively broad waveforms (peak to trough width >300 ms) and a strong tendency to produce complex spike bursts (CSI >3%) whereas putative interneurons had relatively narrow waveforms (peak to trough width <240 ms) and few, if any, complex spike bursts (CSI <3%).

To determine the consequence of CA3-NR1 disruption on the firing of CA3 cells, we measured several electrophysiological properties of hippocampal activity. First, we used two measures to assess the output property of individual CA3 cells, mean firing rate and peak firing rate. Second, we measured the bursting tendencies of hippocampal pyramidal cells using two parameters, burst duration and burst spike frequency (the ratio of number of spikes involved in a burst relative to the total number of spikes produced by a cell). Third, we measured spike width (peak to trough width) as a measure of the intrinsic properties of pyramidal cells.

Local field potential recording from area CA1

Five fNR1, three CA3-Cre mice and 10 mutant mice were employed for local field potential (LFP) recording, during which animals received i.p. injection of 20 mg/kg KA. For mutants receiving KA after DTX pretreatment (n=9), LFP recording was conducted as follows; 30 min recording of background activity, followed by 90 min recording after DTX pretreatment

NIH-PA Author Manuscript

NIH-PA Author Manuscript

NIH-PA Author Manuscript

(0.5 mg/kg, i.p.), followed by over 90 min recording after KA treatment. Because DTX-induced subconvulsive behavioral seizures were observed about 60 min after treatment as previously described (Silveira *et al*., 1988), the last 30-min period before KA treatment was analyzed.

The microwire array consists of eight Formvar-insulated nichrome wires (50 μm in diameter; #762000, AM system, Carlsborg, WA, USA), which were aligned in a single slanted row to vary the depth of recording (1 mm span), with an inter-electrode separation of 100 μm. Each microwire was connected with a silver paint to the pin of an 8-pin subminiature headpiece connector (Mill-Max Mfg. Corp., Oyster Bay, NY, USA) and securely covered by polyester shrink tubing. One pin was bent to attach an enamel-coated copper ground wire (255 μm in diameter) to the skull during the surgery. All the connection points were finally sealed and stabilized with a thin layer of dental acrylic. The impedance of each electrode wire tip was between 0.2 to 0.5 MΩ. The microwire array was surgically-implanted on the skull in the right hemisphere (Stereotaxic coordinates from bregma: 1.7 mm lateral; 2.0 mm posterior; 1.4 mm below the cortical surface at maximum depth) to locate the electrode tips from the corpus callosum to the stratum pyramidale or radiatum of area CA1, and fixed with a ground/reference wire to the skull with cranial screws and dental acrylic. Electrode placement in all animals was confirmed after all the recording procedures were completed, using the histological examination procedures described below. The mice were allowed to recover from anesthesia before returning to their home cages, and were monitored daily for their well-being.

After 10 days recovery from surgery, the microwire array of electrodes was connected to an EIB-27-Micro via a custom-made adaptor, and LFP signals were filtered (bandwidth from 0.1 to 475 Hz), digitized and acquired at a sampling rate of 1.56 kHz per channel using 8 channels of a Cheetah-64 recording system (Neuralynx Inc.). Animals were i.p. injected with KA at 20 mg/kg and LFPs were recorded in a rectangular open arena (24 cm × 18 cm) for 30 min before and for at least 90 min after KA injection. LFP activity monitoring was continued for at least 60 min 1 day (Day 2) and 7 days (Day 8) after injection. For mutants receiving DTX pretreatment, LFP recording was conducted as follows; 30 min recording of background activity, followed by 90 min recording after DTX pretreatment (0.5 mg/kg, i.p.), followed by over 90 min recording after KA treatment. On Days 2 and 8, LFPs were recorded in the same arena used on the day of injection. Because no significant difference was observed in LFP activity between fNR1 and G32-4 Cre mice, the data from both genotypes were combined as a control. On Day 11, the recording sites were micro-lesioned by current injection to verify the location of the recording electrodes, and mice were perfused with 4% formalin for Nissl staining.

KA-induced epileptic activity was obtained from the electrodes placed in CA1 cell layer and analyzed with NeuroExplorer 4 software (Nex Technologies, Littleton, MA, USA). Epileptic discharge in LFP recording was defined by high-frequency and high-voltage synchronous spike activity and/or multi-spike complexes. Epileptiform activity was defined as a brief event of ‘spike and wave’ discharge or ‘burst-like’ discharge with no continuous ictal activity. The duration of epileptiform activity was measured from the onset of initial rise to the point where LFP activity trace returned to baseline with no after-discharge period. LFP activity during an entire recording period was also evaluated with spectrograms in NeuroExplorer 4. To estimate the KA-induced low frequency (30-50 Hz) gamma band oscillations, power spectrum density using Fast Fourier Transformation was analyzed within 2 min before onset of the first epileptic discharge. To calculate the peak power amplitude of gamma band oscillation per animal, we first calculated baseline values of the power spectrum density for each frequency, which was defined as on a linear line between values at the frequencies of 30 Hz and 50 Hz. Peak power amplitude was then measured by

NIH-PA Author Manuscript

NIH-PA Author Manuscript

NIH-PA Author Manuscript

subtracting the baseline value from its peak power value. Data from each animal were analyzed using Statistica 7.0 software (StatSoft Inc., Tulsa, OK, USA).

Off-line analyses of sharp waves (SPW), ripples (R), and theta activity

The LFP signals were analyzed off-line with NeuroExplorer 4 software to visually explore raw signals and calculate spectrograms. The electrode located at the corpus callosum served as a reference electrode. Custom-made software written in a LabView Program (Vernier Software & Technology, Beaverton, OR, USA) was used to detect and analyze SPWs, ripples, and theta activity. Theta and SPW-R containing epochs were independently analyzed after automatic segmentation of the raw signals in >15-sec epochs. Theta activity was defined by calculating the theta/delta power amplitude ratio as previously described (Csicsvari *et al*., 1999). Briefly, Fourier components of the theta (5-10 Hz) and delta (2-4 Hz) frequency bands were calculated in 5-s windows using a Hamming window. Theta activity epochs were analyzed in segments with a theta/delta ratio >6. Mean amplitude and peak-frequency of the theta band was calculated across all epochs per animal. Theta/delta ratios <3 epochs were classified as non-theta periods or SPW-R associated periods and subjected to ripple and SPW detection algorithms. Ripple events were extracted as previously described (Buzsáki *et al*., 2003). The raw signals were digitally filtered (80-250 Hz using a Hamming window-based FIR band-pass digital filter) and background mean and standard deviation (SD) were calculated from the power (root mean square) filtered-signals. Epochs >7 SD from background mean were classified as a ripple; peak-to-trough amplitude was individually measured and averaged for over 100 ripples per animal. In the same time epochs, SPWs were detected in the unfiltered signals by applying a >4 SD background mean exceeding the threshold. Mean-to-trough amplitude was measured for >100 SPWs and averaged per animal. Histograms of SPW peak amplitudes were constructed per animal and averaged for analysis of SPW event distribution across genotypes. In a bimodal event distribution of the mutants obtained, the lower peak corresponded to ‘conventional’ SPW, and a peak exceeding 1.8 mV amplitude was defined as a ‘giant SPW’. In addition, mean-to-trough amplitude and occurrence were separately analyzed for ‘conventional’ and ‘giant’ SPWs.

Statistical Analysis

Data are presented as means and standard errors of the mean (SEMs). N-values are stated in the figure legends. Statistical significance of electrophysiological data between means of experimental and control groups was determined using Student’s *t*-test. Fisher’s exact test and Kruskal-Wallis tests were performed to assess the differences in seizure susceptibility between genotypes. Statistical analysis of immunohistochemical data was performed by Kruskal-Wallis test followed by *post-hoc* with Mann-Whitney test with Bonferroni’s correction for gray value analysis of GABA-IR. Analysis of variance (ANOVA) followed by *post-hoc* Bonferroni test or Tukey test for all other analyses unless otherwise noted. A p-value <0.05 indicates statistical significance.

Results

Reduced firing and impaired spatial representation in mutant CA3 pyramidal cells with hypersynchronous sharp wave-ripple activity

A previous study from our laboratory showed that the place cell activity of CA1 pyramidal cells in a familiar environment in mutant mice was apparently normal (Nakazawa *et al*., 2002). To assess the basic firing and place cell properties of CA3 pyramidal cells in mutant mice, we used an *in vivo* multi-tetrode recording technique in freely moving mice. Multiple single units from hippocampal area CA3 were recorded as animals ran back and forth on a familiar linear track; 24 pyramidal cells from 4 mutants and 20 pyramidal cells from 3 fNR1

NIH-PA Author Manuscript

NIH-PA Author Manuscript

NIH-PA Author Manuscript

controls were quantitatively analyzed. There were dramatic decreases in the mean and peak firing rates of mutant CA3 pyramidal cells compared to those of fNR1 mice (Table 1). The bursting activities of mutant CA3 pyramidal cells, as measured by the duration of a single burst and burst spike frequency—the percentage of spikes that occurred within bursts—also decreased. No difference was observed in peak-to-trough spike width between the genotypes. In addition, we observed defective CA3 place cell activity during animals' exploration in a familiar open arena (Fig. 1), which could be attributed to impaired firing of the mutant CA3 pyramidal cells.

Hypersynchronous SPW-R activity in mutant CA1 during immobility

SPW-R complexes originate in area CA3 and propagate to downstream targets including area CA1 (Chrobak & Buzsáki, 1994,1996;Csicsvari *et al*., 2000;Maier *et al*., 2003;Both *et al*., 2008). To evaluate the effects of CA3 NR1 ablation on CA1 network oscillations, we assessed LFP activity recorded from area CA1 using 7 fNR1 control and 8 mutant mice in a familiar small open arena for 30 min. We first defined theta and irregular slow activity periods by calculating the ratio of the Fourier components of the theta (5-10 Hz) and delta (2-4 Hz) frequency bands (Csicsvari *et al*., 1999). A ratio of >6 SD identified theta periods, and epochs with <3 theta/delta ratio identified SPW-associated irregular slow activity period (Hirase *et al*., 2001). In LFP recordings from the CA1 stratum radiatum where the SPW activity is most robust in mice (Buzsáki *et al*., 2003) (Fig. 2B), the magnitude of mutant SPW activity was overall much higher than that of fNR1 mice during SPW-associated periods (Fig. 2A). Strikingly, the mutant SPW peak amplitudes were invariably bimodally distributed (Fig. 2C), and the larger synchronous population activities exceeding 1.8 mV amplitude, namely 'giant SPW', constituted about 12.7±2.0 % of total SPW events. In contrast, almost no giant SPW activity was observed in the fNR1 control mice in any of the recording periods. The average amplitude of mutant SPWs, excluding 'giant SPWs', was also higher compared to fNR1 controls regardless of the duration of awake immobilization periods (Fig. 2D; amplitude, 1.04±0.05 mV for mutants and 0.78±0.07 mV for fNR1, Student's *t*-test, $P<0.05$). Furthermore, the occurrence of SPWs showed a tendency to increase (0.47±0.07 Hz for mutants and 0.31±0.05 Hz for fNR1, Student's *t*-test, $P=0.09$). Similarly, the averaged amplitude and the occurrence of fast oscillatory ripple activity recorded from CA1 pyramidal cell layer in the mutants were both higher than those of fNR1 controls (Fig. 2, E and F; amplitude, 0.64±0.05 mV for mutants and 0.43±0.07 mV for fNR1, Student's *t*-test, $P<0.05$; occurrence, 0.53±0.03 Hz for mutants and 0.37±0.03 Hz for fNR1, Student's *t*-test, $P<0.005$). These results suggest that NR1 ablation in CA3 pyramidal cells elicits a state of hyper-synchrony in the CA3 recurrent network, which propagates to area CA1 thus generating larger and more frequent SPW-R events. It is also plausible that the reduced firing of mutant CA1 GABAergic cells (Nakazawa *et al*., 2002) contributes to the augmented SPW-R activity in area CA1.

The oscillatory activity during the theta periods in the mutants was normal overall. No differences were observed in the power, peak frequency or the occurrence of theta bands between the genotypes (Fig. 2G). Importantly, no 'giant SPW' events or paroxysmal activities were detected during the theta period, which was consistent with the evidence in the mutants showing normal CA1 place cell activity and spatial learning in the familiar environment (Nakazawa *et al*., 2002,2003) as well as no behavioral seizures induced by audiogenic or tactile stimuli (data not shown). These results suggest that the mutant mice were overall not epileptic.

Mutants were more susceptible to KA-induced seizures

Because KA targets limbic structures and induces epileptic discharges (Ben-Ari *et al*., 1981), we used it to test the long-standing hypothesis that hypersynchronous discharges

NIH-PA Author Manuscript

NIH-PA Author Manuscript

NIH-PA Author Manuscript

reflected in CA3 SPWs play a causal role in the generation of limbic epilepsy (Prince, 1978; Traub & Wong, 1982; Buzsáki, 1986). We first determined that an intraperitoneal (i.p.) injection dose of 20 mg/kg animal body weight of KA induced minimal continuous rearing and falling (‘stage 4′ seizures) and hippocampal damage in fNR1 control mice of B6 background (Fig. S1). Mice of four genotypes received i.p. KA injections—the mutant mouse strain and three control groups: B6 wild-type, fNR1, and G32-4 Cre. Behavioral seizures were evaluated for at least 2 h using a modified Racine’s score (Fig. 3). We found that the latency to ‘stage 3′ seizures was significantly shorter in mutants than in controls, and occurrence of ‘stage 4′ seizures, maximum seizure score, and the cumulative number of seizures were all higher in the mutants than in the control genotypes. Two of the 14 mutants experienced ‘stage 5′ seizures and one of them died after the treatment, while none of the three control genotypes progressed to ‘stage 5′ seizures or died. These results suggest that the mutant mice exhibit an increased susceptibility to KA-induced seizures.

Area CA1 selective neurodegeneration in mutant hippocampus was induced by KA

While the inbred C57BL/6 strain is resistant to neurodegeneration (Schauwecker & Steward, 1997; McKhann *et al*., 2003; McLin & Steward, 2006), increased seizure severity induced by KA treatment may result in increased excitotoxicity in the mutant brain. To evaluate the extent of excitotoxicity induced by KA at the dose of 20 mg/kg, Nissl staining was conducted on parasagittal sections of mutants (Fig. 4, A and B) and fNR1 controls (Fig. S2, A and B) that manifested ‘stage 4′ or more severe seizures during the first 2-h period after treatment. In the hippocampus of mutants 1 day after KA injection, we observed extensive excitotoxic alterations as revealed by highly condensed pyknotic nuclei in the CA1 cell layer, but not in the CA2/CA3 or dentate gyrus (Fig. 4B). Four weeks after KA injection, extensive cell loss was prominent in the CA1 pyramidal cell layer of mutants, while no apparent degeneration was observed in the CA2/CA3 cell layer or dentate granule cell layer. In contrast, almost no hippocampal cell loss was detected in the fNR1 mice in any subfield at any stage following KA administration (Fig. S2B). Because the results in B6 wild-type and G32-4 Cre mice were almost identical to those observed in fNR1 mice, we used the results from fNR1 mice as the control genotype in all subsequent histological analyses.

To detect KA-induced neurodegeneration with higher sensitivity, fNR1 and mutant mice underwent KA i.p. treatment and brain sections were processed for neurosilver staining. Consistent with Nissl staining, most CA1 pyramidal cells were silver-stained from 1 day to 1 wk after KA treatment in all the mutants that manifested ‘stage 4′ or more severe seizures (graph in Fig. 4C, $F_{(3,32)}=27.62$ for genotype × time interaction in CA1, $P<0.00001$, untreated mutant vs mutant at 1 day and 7 days after KA treatment, $P<0.0005$; fNR1 vs mutant at 1 day and 7 days after KA treatment, $P<0.0005$). In contrast, almost no silver impregnated cells were observed in area CA2/3, dentate gyrus, subiculum, entorhinal cortex, or lateral septum (Fig. S2, C-F), suggesting that these brain areas are unlikely to be KA-induced epileptic loci in the mutants. These stained cells largely disappeared within 4 wk after treatment, probably due to immunological clearance of dead cells. In contrast, in control fNR1 mice, almost no staining was found in any brain area, despite that fact that some mice had shown equivalent stages of KA-induced seizure. To confirm the KA-induced neurodegeneration, sections from both genotypes were stained with Fluoro-Jade B, a high affinity fluorescent marker for the localization of neuronal degeneration (Schmued & Hopkins, 2000). In the mutant hippocampus, distribution of Fluoro-Jade B stained cells largely coincided with the silver impregnated cells, confirming that neurodegeneration was localized to area CA1 in the mutant hippocampus (Fig. 4E).

To further elucidate this issue, we examined whether seizure severity correlated with KA-induced excitotoxic cell damage in the hippocampus. We used Nissl staining for morphological analyses of fNR1 (n=30) and mutant (n=29) mice 1 to 4 wk after KA

NIH-PA Author Manuscript

NIH-PA Author Manuscript

NIH-PA Author Manuscript

treatment, including the mice depicted in Fig. 3 and Fig. 4, A-C. Figure 4D shows 3-D histogram plots of the maximum seizure score for the first 2 h after KA treatment, compared to subsequent damage in the CA1 cell layer for each genotype. Mutants showed a clear correlation between the severity of seizure and the extent of CA1 cell damage, but the two scores were not correlated in fNR1 controls (Pearson coefficient for mutant, r=0.74, P<0.00005; Pearson coefficient for fNR1, r=0.27, P=0.14; genotype effect, P<0.05). Furthermore, the mutant damage scores were bimodally distributed, and about 40% of mutants with less severe seizure scores exhibited no CA1 degeneration. In contrast, most fNR1 mice (28 out of 30) showed CA1 cell death regardless of the severity of seizure scores.

KA-induced epileptic discharges with attenuated gamma oscillation in area CA1 of mutants

To explore the underlying mechanisms by which CA3 NR1 ablation resulted in KA-induced excitotoxic cell death in area CA1, we assessed LFP activity in the CA1. LFP recordings were performed during the first 90 min, 1 and 7 days after KA injection, using electrodes implanted into the dorsal area CA1 in fNR1 (n=5) and Cre (n=3) control mice and in mutant mice (n=10). All of the KA-treated animals carrying a microwire array exhibited typical behavioral seizures, similar to those described in Fig. 5A, lasting several hours and subsiding spontaneously on that day. Because the results from fNR1 and Cre mice were almost identical, these results were combined and treated as a “control” genotype. During the acute phase, highly synchronous epileptic discharges repeatedly occurred in area CA1 of both control (trace #1) and mutant (traces #3 and #5) mice (Fig. 5A). The latency to epileptic discharges after KA injection was significantly shorter in mutants than in control mice (Fig. 5B). The occurrence of epileptic discharge events during the first 90 min after KA treatment was also higher in mutants (Fig. 5C). Cumulative epileptic discharge duration during this period was also longer in mutants than controls (Fig. 5D). It is conceivable that the magnitude of mutant epileptic discharges could contribute to CA1 neurodegeneration. In fact, when mutants were subdivided into two groups according to the CA1 damage score shown in the middle panel of Fig. 9A, the magnitude of epileptic discharge events was much more robust in the mutants that eventually showed cell death in area CA1 (Group B) compared to those that did not (Group A) (Fig. 5, C and D).

In control mice, another prominent KA-induced oscillatory activity was low-frequency (30-50 Hz) gamma band oscillation that appeared approximately 15-20 min after KA injection and 10 min before the onset of the first epileptic discharge (trace #2 in Fig. 5, A and E). This is consistent with reports of KA-induced 30-40 Hz oscillatory synchronous activity in the rodent hippocampus *in vivo* (Medvedev *et al*., 2000; Khazipov & Holmes, 2003; Sakatani *et al*., 2008). However, the LFP power spectrogram of mutant CA1 (Fig. 5F) revealed a significantly lower magnitude of 30-50 Hz gamma band oscillations during this period in the mutants than in the controls (trace #6 in Fig. 5, A and E). Remarkably, KA-induced gamma band oscillatory activity almost disappeared in Group B mutants (those with cell death); in contrast, this activity remained observable in Group A mutants (those without cell death; Fig. 5G). Because Group A mutants exhibited gamma oscillations despite a short latency to epileptic discharges (Fig. 5B), this effect in Group B mutants did not appear to be due to obscured detection of gamma oscillations by epileptic discharges. These results suggest that the magnitude of 30-50 Hz gamma oscillations before onset of epileptic discharges was inversely correlated with the degree of CA1 excitotoxicity.

Epileptiform activity was sustained in mutant CA1

To further explore the process leading to CA1 neurodegeneration in the mutants, LFP recording was continued on the day following KA injection. LFP activity in the CA1 area of fNR1 or Cre control mice showed no continuous ictal discharges and was almost

NIH-PA Author Manuscript

NIH-PA Author Manuscript

NIH-PA Author Manuscript

indistinguishable to that observed before KA treatment. However, area CA1 in the mutants exhibited epileptiform activity characteristic of large-amplitude spike-like discharges on Day 2 (Fig. 6A), although they displayed no continuous ictal discharges. Among mutants, Group A (non-cell death) mutant mice displayed 'spike and wave' discharges superimposed upon normal background activity. In contrast, Group B mutant mice, having undergone massive CA1 degeneration, showed polyspike discharges with longer durations on top of the suppressed background activity. Quantitative analysis revealed that the occurrence of such epileptiform activity, which was rarely observed in the controls, was higher in Group B than Group A mutants (Fig. 6B). The duration of individual epileptiform activity was also longer in Group B mutants (Fig. 6C). Remarkably, polyspike discharge-type epileptiform activity was still present in Group B mutants at least 7 days after KA treatment, whereas simple 'spike and wave' discharges were rarely observed in Group A mutants (Fig. 6D). These results suggest that the massive CA1 neurodegeneration observed in Group B mutants resulted from the polyspike discharge-type epileptiform activity observed on Day 2.

KA-induced degeneration of mutant CA1 GABAergic cells

Attenuation of low frequency gamma oscillations in the acute phase and the subsequent epileptiform activity on the following days in the group B mutants could reflect a deficit in CA1 GABAergic network activity upon KA administration. To evaluate the integrity of hippocampal GABAergic networks, we quantified the neurosilver-positive cells in the mutant CA1 subfield in neurosilver-stained sections shown in Fig. 4C. Prominent increases in neurosilver-positive cells were observed not only in the cell layer (stratum pyramidale) but also in other strata 1 day after KA treatment (Fig. 7A), suggesting neurodegeneration of CA1 interneurons. Fluoro Jade-B positive sections (Fig. 4E) were also immunostained with anti-GAD67, the GABA synthesizing enzyme, and double-labeling confirmed degeneration of mutant GABAergic interneurons in area CA1 (Fig. 7B).

To further examine the extent of the damage to the degenerated interneurons, we quantified the GAD67-positive cells in untreated and KA-treated animals which showed 'stage 4′ or more severe seizures (Fig. 7C). The number of GAD67-positive cells in CA1 of fNR1 control mice decreased 1 day after KA treatment but returned to the levels seen in untreated mice within 1 wk (Fig. 7D). In contrast, the number of GAD67-positive cells in the CA1 subfield of the mutants decreased to less than 50% of fNR1 control mice 1 day after injection and was unchanged 4 wk after treatment. In the mutants, regional analysis revealed a severe and permanent KA-induced reduction of GAD67-positive cells in all strata compared with fNR1 mice, except for cells in the lacunosum-moleculare (Fig. 7E). Notably, the total number of GAD67-positive cells in stratum oriens (~150 cells/mm^2) and stratum radiatum (~50 cells/mm^2) (see 'untreated' cell number in Fig. 7E) was similar to the number of mutant neurosilver-positive cells in the same strata 1 day after KA treatment (Fig. 7A), suggesting that while most GABAergic neurons in the mutants transiently suffered neurodegeneration upon KA administration, at least 60% of GABAergic cells in these CA1 strata permanently lost GAD67-IR, presumably coinciding with cell death. On the other hand, the number of mutant neurosilver-positive cells in stratum lacunosum-moleculare (~50 cells/mm^2) was far less than the total number of GAD67-positive cells in the same strata (~200 cells/mm^2). Their GAD67 activity was also largely restored 1 wk after KA treatment. Because the main input to lacunosum-moleculare interneurons comes from the entorhinal cortex (Klausberger & Somogyi, 2008) (not from the CA3), the results suggest that CA1 GABAergic cells receiving reduced output selectively from CA3 suffered severe neurodegenerative change upon KA treatment.

NIH-PA Author Manuscript

NIH-PA Author Manuscript

NIH-PA Author Manuscript

Pretreatment with DTX restored mutant KA-induced gamma oscillation, GAD67 activity, and resistance to CA1 neurodegeneration

GABAergic interneuron activity suppresses excitotoxicity during seizures (Ylinen *et al*. 1991; Mody, 1998). Therefore, we wondered whether boosting GABA levels before the onset of the first seizure discharge could protect against CA1 neurodegeneration in the mutants. To test this, we used DTX, a D-type potassium channel blocker, because it acts on presynaptic voltage-gated potassium channels of cortical interneurons (Weller *et al*., 1985; Richards *et al*., 2000; Cunningham & Jones, 2001; Shimada *et al*., 2007) and is a potent enhancer of presynaptic GABA release. The extent to which DTX pretreatment affected presynaptic release was assessed by anti-GABA-IR in the CA1 cell layer where axon terminals of GABAergic interneurons exuberantly arborize. We first confirmed that there were no obvious effects of a subconvulsive dose of DTX (0.5 mg/kg i.p.) prior to KA treatment on the CA1 SPW-R activity in the mutants (Fig. 8). This was not surprising because SPW-R activity is generated in area CA3 where GABAergic function seemed to be normal in the mutants (Fig. S3).

We then evaluated several parameters for LFP activity and CA1 excitotoxicity by injecting KA 90 min after DTX pretreatment. Fig. 9A shows the histograms of behavioral seizure scores for each animal after KA injection as well as the CA1 damage score 10 days after the treatment. We found that the behavioral seizure score (Fig. 9B) as well as the number and duration of mutant epileptic discharges (Fig. 9C) were not affected by DTX-pretreatment, which was unexpected. Furthermore, the damage scores in DTX-pretreated mutants were dramatically lower than in saline-pretreated mutants (Fig. 9, A and B). Remarkably, DTX pretreatment in mutants also evoked robust low frequency gamma oscillations before the onset of seizure discharges (Fig. 10A, trace #1 for seizure discharge and trace #2 for gamma oscillation), and the magnitude of gamma oscillations was equivalent to those observed in fNR1 or Cre control mice (Fig. 10B), suggesting that DTX-sensitive, voltage-gated potassium channels are instrumental in synchronizing KA-induced gamma oscillations.

In parallel, KA-induced GABA increases were assessed by comparing GABA-IR levels in CA1 to the IR level of the corpus callosum where few GABAergic cells are localized (Fig. 10, C and D). GABA-IR levels in the CA1 cell layer 20 min after KA treatment were significantly higher than in the corpus callosum in controls, which is consistent with previous reports demonstrating KA-induced GABA release in the hippocampus (Zhang *et al*., 1990; Ding *et al*., 1998). Remarkably, the CA1 cell layer in mutants showed no increased GABA levels in response to KA injection and this was significantly rescued by pretreatment with DTX. The deficit in KA-induced GABA increases appeared to be specific to area CA1 in mutants because no difference was observed in other subfields.

To further evaluate the effects of DTX-induced gamma oscillations on subsequent days, the peak power amplitude of gamma oscillations and the occurrence of epileptiform activity on Day 2 were plotted for all the animals, including the mutants pretreated with DTX (Fig. 10E). We found that the number (Fig. 10E) and duration (Fig. 10F) of epileptiform activity in the pretreated mutants was decreased compared to the saline-pretreated mutants. Moreover, the number of CA1 GAD67-positive cells in mutants was also equivalent to that found in fNR1 mice 1 wk later (Fig. 10G), suggesting that DTX-induced low frequency gamma band oscillations restored CA1 GABAergic cell function. Accordingly, 10 days after DTX and KA treatment, almost no CA1 degeneration was observed in the mutants as revealed by Neurosilver staining (Fig. 9B).

NIH-PA Author Manuscript

NIH-PA Author Manuscript

NIH-PA Author Manuscript

DISCUSSION

The present study had several salient findings. Specifically, (1) CA3-NR1 KO mutants displayed reduced CA3 pyramidal cell firing, impaired CA3 spatial representation, and augmented SPW-R activity; (2) systemic KA administration to the mutants resulted in impaired KA-induced GABAergic activation and 30-50 Hz gamma oscillations. These were accompanied by augmented seizure discharges, thereby leading to massive and strikingly selective neurodegeneration in area CA1; (3) in the mutants, the magnitude of KA-induced gamma oscillations was inversely correlated with the magnitude of epileptiform activity, the degree of CA1 degeneration, and the viability of GAD67-positive cells in the days following KA treatment; and (4) pretreatment with DTX, which restored CA1 GABA levels, maintained mutant KA-induced gamma oscillations and GAD67-positivity, thereby preventing the mutant CA1 cells from excitotoxic cell death. Taken together, the results indicate that a lack of KA-induced gamma oscillations before onset of seizure discharges correlates with prolonged seizure activity and CA1 excitotoxicity, suggesting that persistent gamma oscillations predict resilience to excitotoxic insults.

Increased susceptibility to KA-induced seizure and CA1 excitotoxicity following CA3 NR1 ablation

To explore the relationship between gamma oscillations and excitotoxicity, it was essential to employ CA3-NR1 KO mice (referred to as “mutants” throughout this manuscript). In these mice, two possibly interrelated events were observed following genetic NR1 ablation of CA3 pyramidal cells during adulthood (Nakazawa *et al*., 2002)—a dramatic decrease in CA3 pyramidal cell firing/bursting and augmented SPW-R activity. It is not obvious how functional ablation of CA3 NRs could decrease action potential generation. In fact, firing rates of CA1 pyramidal cells lacking the same NR1 subunit were almost the same as those of control mice (McHugh *et al*., 1996). The results obtained here could simply be due to the mutual reduction of afferent drive from nearby CA3 pyramidal cells as well as the inhibition of cell firing by CA3 interneurons (Freund & Buzsáki, 1996). Another possibility, which is not mutually exclusive, is that CA3 NRs could contribute to normal excitatory synaptic transmission, as described in adult visual cortex (Miller *et al*., 1989), sensory thalamus (Kemp & Sillito, 1982; Salt, 1986) and the red nucleus (Davies *et al*., 1986), or could even contribute to action potential generation (Zhao *et al*., 2005).

On the other hand, increased SPW-R activity during immobility is paradoxical given that CA3 recurrent network activity is low since generation of CA3 SPW-R apparently requires CA3 recurrent network activity (Csicsvari *et al*., 2000; Behrens *et al.*, 2005). While NR antagonists prevent the induction of the SPW-R complex (Behrens *et al.*, 2005), NRs seem to be unnecessary for maintaining spontaneous SPW-Rs once the SPW-Rs are established (Behrens *et al.*, 2005) or in the ventral portions of the hippocampal CA3 where spontaneous SPW-Rs are observed (Maier *et al*., 2003; Papatheodoropoulos & Kostopoulos, 2002; Colgin *et al*., 2004). Rather, the magnitude of CA3 SPW-Rs nearly doubled following the application of an NR antagonist in rat slices, perhaps via mechanisms that involve decreased Ca^{2+} influx through NRs and a subsequent inactivation of SK type2 Ca^{2+}-activated potassium channels mediating afterhyperpolarization (Colgin *et al*., 2004). Because CA3 NR1 was eliminated along the longitudinal axis including ventral CA3 in the mutants (Nakazawa *et al*., 2002), spontaneous SPW-Rs could become larger in ventral CA3 after postadolescent NR1 ablation, subsequently spreading to dorsal CA3 and further to area CA1. While the mechanisms underlying the generation of spontaneous ‘giant SPWs’ are unknown, impaired Ca^{2+}-activated afterhyperpolarization could play a role because its abnormal regulation may contribute to epileptiform discharges (Fernández de Sevilla *et al*., 2006). Alternatively, ‘giant SPWs’ could be a consequence of decreased CA3 pyramidal cell

NIH-PA Author Manuscript

NIH-PA Author Manuscript

NIH-PA Author Manuscript

firing because spontaneous oscillatory bursting seems to be a common behavior of tetrodotoxin (TTX)-treated neurons (Ramakers *et al*., 1990; Trasande & Ramirez, 2007).

Consequently, in this study, the mutants displayed increased susceptibility to KA-induced seizures and CA1 excitotoxicity, due to impaired GABAergic function in area CA1 of the hippocampus, and abnormally high SPW-R activity during periods of immobility. One plausible explanation for the remarkably selective CA1 neurodegeneration seen here is that reduced afferent drive from CA3 to CA1 interneurons in a feed-forward manner leads to a coherent loss of postsynaptic inhibition in area CA1 upon KA treatment, thus rendering CA1 cells vulnerable to excitotoxicity. Interestingly, almost no CA3 cell death in mutants was observed despite reduced afferent drive from the recurrent network.

The KA dose used here for systemic injection (20 mg/kg i.p.) was instrumental in determining the cellular process by which KA injection led to neurodegeneration of mutant CA1 cells. Approximately half of the mutants manifested massive and irreversible cell loss in the CA1 cell layer; in contrast, the other half displayed almost no cell death (Figs. 4D and 9A). This non-cell death group (Group A mutants) became an excellent animal control in the same genotype to evaluate the process of CA1 degeneration for the Group B mutants. The high variability to KA-induced excitotoxicity among the mutants could be due to that the KA dose used, 20 mg/kg, is close to the threshold dose to evoke the clonic seizures (‘stage 3′ seizure or more, Fig. S1).

KA-evoked GABA release to generate gamma oscillations, preventing CA1 excitotoxicity

Systemic KA injection increases extracellular GABA levels in rodent hippocampus (Zhang *et al*., 1990; Ding *et al*., 1998), which could be attributed to direct KA action on GluR5-containing KA receptors that are located on presynaptic axon terminals of interneurons and release GABA (Khalilov *et al*., 2002; Fisahn *et al*., 2004). In the present study, KA injection in mutants did not increase GABA levels or trigger gamma oscillations in area CA1 in the same way as in control animals. However, it is possible that chronic reduction of afferent drives from the CA3 area of mutants could result in KA-induced deficiencies in GABA release from CA1 interneurons. To rescue this deficit, we used DTX, a potent enhancer of presynaptic GABA release. DTX is a selective blocker of $_{D}$-type voltage-gated potassium channels ($Kv_{1.1}$, $Kv_{1.2}$, and $Kv_{1.6}$) (Judge & Bever, 2006) and stimulates GABA release in rat cortical synaptosome fractions (Weller *et al*., 1985), rat entorhinal cortex (Cunningham & Jones, 2001), and substantia nigra (Shimada *et al*., 2007); glutamate release action seems to be weak in rat hippocampus (Richards *et al*., 2000) and entorhinal cortex (Cunningham & Jones, 2001). As expected, administration of DTX prior to KA treatment restored the CA1 GABA levels in the area CA1 but, remarkably, preserved KA-induced gamma oscillations. Released GABA, in turn, stimulates the $GABA_A$ receptors of other GABAergic cells and/or CA1 pyramidal cells, maintaining KA-triggered gamma oscillations (Bartos *et al*., 2007; Mann & Paulsen, 2007). In fact, a recent study provides firm evidence that gamma oscillations arise from a network of mutually connected fast-spiking GABAergic neurons (Cardin *et al*., 2009). Therefore, restoration of gamma oscillations in area CA1 by DTX treatment could be attributed to an enhanced GABA release, regardless of DTX actions on other neurotransmitters. Interestingly, KA-induced extracellular secretion of the calcium-binding protein S100B from astrocytes has recently been shown to enhance KA-induced gamma oscillations (Sakatani *et al*., 2008). Therefore, we cannot exclude the possibility that other mechanisms enhance the gamma oscillations upon KA administration.

Status epilepticus has long been implicated in brain damage, and several studies suggest a positive association between adverse outcomes and duration of status epilepticus (Norman, 1964; Corsellis & Bruton, 1983). In this study, we found that DTX pretreatment did not alter the magnitude of KA-induced seizure discharges, possibly due to the influence of enhanced

NIH-PA Author Manuscript

NIH-PA Author Manuscript

NIH-PA Author Manuscript

SPW-R activity in the mutants. Therefore, KA-induced seizure severity during the first 2 h of status epilepticus did not necessarily determine the magnitude of excitotoxicity. In contrast, protection from excitotoxicity by pretreatment with DTX, accompanied by the re-emergence of persistent gamma oscillations, suggests that KA-induced GABA release is critical for the prevention of CA1 neurodegeneration. Furthermore, DTX pretreatment also significantly suppressed KA-induced epileptiform activity the following day. This suggests that KA-induced GABA release by DTX pretreatment may prevent the initiation of subsequent processes leading to excitotoxicity, including epileptiform activity, on the following day (Fig. 11).

Clinical implications

What is more important in this study is that the magnitude of low frequency gamma oscillations prior to the onset of behavioral seizures was inversely correlated with the occurrence of epileptiform activity on subsequent days (Fig. 10E). This is a finding of considerable clinical importance, because persistent gamma oscillations, which are measurable via EEG recordings in humans, could be used as an alternative prognostic indicator for predicting resilience to excitotoxicity. Interestingly, the prognostic value of oscillatory activity for seizure outcomes may vary, depending on the oscillation frequencies. Fast gamma (60-100 Hz) oscillations have been reported to predict the development of ictal seizures in human neocortical epilepsy patients (Worrell *et al*., 2004). In contrast, 'low-voltage fast activity' (>13 Hz), beta (15-30 Hz), or gamma frequency in the neocortex were more prevalent in favorable outcome groups after resective surgery (Lee *et al*., 2000;Park *et al*., 2002). The present findings predicted not only a good prognostic value of hippocampal low frequency gamma oscillations for prolonged epileptiform activity but also excitotoxicity. Whether the identification of low frequency gamma oscillations could be of prognostic value in the treatment of epilepsy patients remains unknown, but clearly warrants further research.

The use of cell-type specific transgenic mutants also demonstrated that CA3 pyramidal cell-specific alterations are capable of initiating epilepsy after excitotoxic insults. It has long been suspected that the CA3 recurrent network is one of the critical loci in medial temporal lobe epilepsy (Buzsáki, 1986; Traub *et al*., 1989). Recently, Nosten-Bertrand and colleagues (Nosten-Bertrand *et al.*, 2008) reported that a dysplastic CA3 subfield in hippocampal slices of doublecortin (Dcx) knockout mice generates SPW-like spontaneous activity and increases susceptibility to epilepsy. Interestingly, Dcx mutations in humans cause type I lissencephaly to subcortical laminar heterotopia (SCLH), which are associated with epilepsy (Guerrini & Marini, 2006). While it is unclear to what extent Dcx mutation-derived defects are confined to the CA3 subfield in SCLH patients, the present study, along with these recent clinical data, suggest that the CA3 subfield may indeed be a site of epileptogenesis in humans.

Supplementary Material

Refer to Web version on PubMed Central for supplementary material.

Acknowledgments

We thank Dr. Linus D. Sun and Ms. Catherine J. Cravens for technical assistance, Drs. Brian Condie and John Rubenstein for providing GAD67 cDNA plasmid, and Drs. György Buzsáki, Dax Hoffman, Karen N. Gale, Brita Fritsch, Kim Christian, and Ioline Henter for valuable advice and critical reading of this manuscript. This research was supported by the Intramural Research Program of the National Institute of Mental Health and by NIH Grant R01-MH078821 to ST. SJ was supported in part by a Japan Society for the Promotion of Science (JSPS) fellowship.

NIH-PA Author Manuscript

NIH-PA Author Manuscript

NIH-PA Author Manuscript

Abbreviations

B6	C57BL/6
DTX	α-dendrotoxin
fNR1	floxed-NR1
GABA	γ-Aminobutyric acid
GAD67	67-kDa isoform of glutamic acid decarboxylase
IR	immunoreactivity
KA	kainic acid
LFP	local field potential
SPW-R	sharp wave-ripple

References

Alarcon G, Binnie CD, Elwes RD, Polkey CE. Power spectrum and intracranial EEG patterns at seizure onset in partial epilepsy. Electroencephalogr. Clin. Neurophysiol. 1995; 94:326–337. [PubMed: 7774519]

Allen PJ, Fish DR, Smith SJ. Very high-frequency rhythmic activity during SEEG suppression in frontal lobe epilepsy. Electroencephalogr. Clin. Neurophysiol. 1992; 82:155–159. [PubMed: 1370786]

Bartos M, Vida I, Jonas P. Synaptic mechanisms of synchronized gamma oscillations in inhibitory interneuron networks. Nat. Rev. Neurosci. 2007; 8:45–56. [PubMed: 17180162]

Behrens CJ, van den Boom LP, de Hoz L, Friedman A, Heinemann U. Induction of sharp wave-ripple complexes in vitro and reorganization of hippocampal networks. Nat. Neurosci. 2005; 8:1560–1567. [PubMed: 16222227]

Ben-Ari Y, Tremblay E, Riche D, Ghilini G, Naquet R. Electrographic, clinical and pathological alterations following systemic administration of kainic acid, bicuculline or pentetrazole: metabolic mapping using the deoxyglucose method with special reference to the pathology of epilepsy. Neuroscience. 1981; 6:1361–1391. [PubMed: 7266871]

Ben-Ari Y. Limbic seizure and brain damage produced by kainic acid: mechanisms and relevance to human temporal lobe epilepsy. Neuroscience. 1985; 14:375–403. [PubMed: 2859548]

Both M, Bähner F, von Bohlen, Halbach O, Draguhn A. Propagation of specific network patterns through the mouse hippocampus. Hippocampus. 2008; 18:899–908. [PubMed: 18493949]

Bragin A, Engel J Jr, Wilson CL, Vizentin E, Mathern GW. Electrophysiologic analysis of a chronic seizure model after unilateral hippocampal KA injection. Epilepsia. 1999; 40:1210–1221. [PubMed: 10487183]

Buzsáki G. Hippocampal sharp waves: their origin and significance. Brain Res. 1986; 398:242–252. [PubMed: 3026567]

Buzsáki G, Buhl DL, Harris KD, Csicsvari J, Czéh B, Morozov A. Hippocampal network patterns of activity in the mouse. Neuroscience. 2003; 116:201–211. [PubMed: 12535953]

Buzsáki G, Draguhn A. Neuronal oscillations in cortical networks. Science. 2004; 304:1926–1929. [PubMed: 15218136]

Cardin JA, Carlén M, Meletis K, Knoblich U, Zhang F, Deisseroth K, Tsai LH, Moore CI. Driving fast-spiking cells induces gamma rhythm and controls sensory responses. Nature. 2009; 459:663–667. [PubMed: 19396156]

Chrobak JJ, Buzsáki G. Selective activation of deep layer (V-VI) retrohippocampal cortical neurons during hippocampal sharp waves in the behaving rat. J. Neurosci. 1994; 14:6160–6170. [PubMed: 7931570]

Chrobak JJ, Buzsáki G. High-frequency oscillations in the output networks of the hippocampal-entorhinal axis of the freely behaving rat. J. Neurosci. 1996; 16:3056–3066. [PubMed: 8622135]

NIH-PA Author Manuscript

NIH-PA Author Manuscript

NIH-PA Author Manuscript

Colgin LL, Kubota D, Brucher FA, Jia Y, Branyan E, Gall CM, Lynch G. Spontaneous waves in the dentate gyrus of slices from the ventral hippocampus. J. Neurophysiol. 2004; 92:3385–3398. [PubMed: 15282260]

Corsellis JA, Bruton CJ. Neuropathology of status epilepticus in humans. Adv. Neurol. 1983; 34:129–139. [PubMed: 6829328]

Csicsvari J, Hirase H, Czurkó A, Mamiya A, Buzsáki G. Oscillatory coupling of hippocampal pyramidal cells and interneurons in the behaving Rat. J. Neurosci. 1999; 19:274–287. [PubMed: 9870957]

Csicsvari J, Hirase H, Mamiya A, Buzsáki G. Ensemble patterns of hippocampal CA3-CA1 neurons during sharp wave-associated population events. Neuron. 2000; 28:585–594. [PubMed: 11144366]

Cunningham MO, Jones RS. Dendrotoxin sensitive potassium channels modulate GABA but not glutamate release in the rat entorhinal cortex in vitro. Neuroscience. 2001; 107:395–404. [PubMed: 11718995]

Davies J, Miller AJ, Sheardown MJ. Amino acid receptor mediated excitatory synaptic transmission in the cat red nucleus. J. Physiol. 1986; 376:13–29. [PubMed: 2879036]

Ding RG, Asada H, Obata K. Changes in extracellular glutamate and GABA levels in the hippocampal CA3 and CA1 areas and the induction of glutamic acid decarboxylase-67 in dentate granule cells of rats treated with kainic acid. Brain Res. 1998; 800:105–110. [PubMed: 9685600]

Fernández de Sevilla D, Garduño J, Galván E, Buño W. Calcium-activated afterhyperpolarizations regulate synchronization and timing of epileptiform bursts in hippocampal CA3 pyramidal neurons. J. Neurophysiol. 2006; 96:3028–3041. [PubMed: 16971683]

Fisahn A, Contractor A, Traub RD, Buhl EH, Heinemann SF, McBain CJ. Distinct roles for the kainate receptor subunits GluR5 & GluR6 in kainate-induced hippocampal gamma oscillations. J. Neurosci. 2004; 24:9658–9668. [PubMed: 15509753]

Fisher RS, Webber WR, Lesser RP, Arroyo S, Uematsu S. High-frequency EEG activity at the start of seizures. J. Clin. Neurophysiol. 1992; 9:441–448. [PubMed: 1517412]

Freund TF, Buzsáki G. Interneurons of the hippocampus. Hippocampus. 1996; 6:347–470. [PubMed: 8915675]

Guerrini R, Marini C. Genetic malformations of cortical development. Exp. Brain Res. 2006; 173:322–333. [PubMed: 16724181]

Hirase H, Leinekugel X, Csicsvari J, Czurkó A, Buzsáki G. Behavior-dependent states of the hippocampal network affect functional clustering of neurons. J. Neurosci. 2001; 21(RC145):1–4.

Hughes JR. Gamma, fast, and ultrafast waves of the brain: their relationships with epilepsy and behavior. Epilepsy Behav. 2008; 13:25–31. [PubMed: 18439878]

Jirsch JD, Urrestarazu E, LeVan P, Olivier A, Dubeau F, Gotman J. High-frequency oscillations during human focal seizures. Brain. 2006; 129:1593–608. [PubMed: 16632553]

Judge SI, Bever CT Jr. Potassium channel blockers in multiple sclerosis: neuronal Kv channels and effects of symptomatic treatment. Pharmacol. Ther. 2006; 111:224–259. [PubMed: 16472864]

Kemp JA, Sillito AM. The nature of the excitatory transmitter mediating X and Y cell inputs to the cat dorsal lateral geniculate nucleus. J. Physiol. 1982; 323:377–391. [PubMed: 6124634]

Khalilov I, Hirsch J, Cossart R, Ben-Ari Y. Paradoxical anti-epileptic effects of a GluR5 agonist of kainate receptors. J. Neurophysiol. 2002; 88:523–527. [PubMed: 12091575]

Khazipov R, Holmes GL. Synchronization of kainate-induced epileptic activity via GABAergic inhibition in the superfused rat hippocampus in vivo. J. Neurosci. 2003; 23:5337–5341. [PubMed: 12832559]

Klausberger T, Somogyi P. Neuronal diversity and temporal dynamics: the unity of hippocampal circuit operations. Science. 2008; 321:53–57. [PubMed: 18599766]

Lee SA, Spencer DD, Spencer SS. Intracranial EEG seizure-onset patterns in neocortical epilepsy. Epilepsia. 2000; 41:297–307. [PubMed: 10714401]

Maier N, Nimmrich V, Draguhn A. Cellular and network mechanisms underlying spontaneous sharp wave-ripple complexes in mouse hippocampal slices. J. Physiol. 2003; 550:873–887. [PubMed: 12807984]

NIH-PA Author Manuscript

NIH-PA Author Manuscript

NIH-PA Author Manuscript

Mann EO, Paulsen O. Role of GABAergic inhibition in hippocampal network oscillations. Trends Neurosci. 2007; 30:343–349. [PubMed: 17532059]

McHugh TJ, Blum KI, Tsien JZ, Tonegawa S, Wilson MA. Impaired hippocampal representation of space in CA1-specific NMDAR1 knockout mice. Cell. 1996; 87:1339–1349. [PubMed: 8980239]

McKhann GM, Wenzel HJ, Robbins CA, Sosunov AA, Schwartzkroin PA. Mouse strain differences in kainic acid sensitivity, seizure behavior, mortality, and hippocampal pathology. Neuroscience. 2003; 122:551–561. [PubMed: 14614919]

McLin JP, Steward O. Comparison of seizure phenotype and neurodegeneration induced by systemic kainic acid in inbred, outbred, and hybrid mouse strains. Eur. J. Neurosci. 2006; 24:2191–2202. [PubMed: 17074044]

Medvedev A, Mackenzie L, Hiscock JJ, Willoughby JO. Kainic acid induces distinct types of epileptiform discharge with differential involvement of hippocampus and neocortex. Brain Res. Bull. 2000; 52:89–98. [PubMed: 10808078]

Medvedev AV. Temporal binding at gamma frequencies in the brain: paving the way to epilepsy? Australas. Phys. Eng. Sci. Med. 2001; 24:37–48. [PubMed: 11458571]

Miller KD, Chapman B, Stryker MP. Visual responses in adult cat visual cortex depend on N-methyl-D-aspartate receptors. Proc. Natl. Acad. Sci. U.S.A. 1989; 86:5183–5187. [PubMed: 2567996]

Mody I. Ion channels in epilepsy. Annu. Rev. Pharmacol. Toxicol. 1998; 38:321–350. [PubMed: 9597158]

Nadler JV. Minireview. Kainic acid as a tool for the study of temporal lobe epilepsy. Life Sci. 1981; 29:2031–2042. [PubMed: 7031398]

Nakazawa K, Quirk MC, Chitwood RA, Watanabe M, Yeckel MF, Sun LD, Kato A, Carr CA, Johnston D, Wilson MA, Tonegawa S. Requirement for hippocampal CA3 NMDA receptors in associative memory recall. Science. 2002; 297:211–218. [PubMed: 12040087]

Nakazawa K, Sun LD, Quirk MC, Rondi-Reig L, Wilson MA, Tonegawa S. Hippocampal CA3 NMDA receptors are crucial for memory acquisition of one-time experience. Neuron. 2003; 38:305–315. [PubMed: 12718863]

Norman RN. The neuropathology of status epilepticus. Med. Sci. Law. 1964; 4:45–61.

Nosten-Bertrand M, Kappeler C, Dinocourt C, Denis C, Germain J, Tuy F. Phan Dinh, Verstraeten S, Alvarez C, Métin C, Chelly J, Giros B, Miles R, Depaulis A, Francis F. Epilepsy in Dcx knockout mice associated with discrete lamination defects and enhanced excitability in the hippocampus. PLoS ONE. 2008; 3:e2473. [PubMed: 18575605]

Papatheodoropoulos C, Kostopoulos G. Spontaneous GABA(A)-dependent synchronous periodic activity in adult rat ventral hippocampal slices. Neurosci.Lett. 2002; 319:17–20. [PubMed: 11814643]

Park SA, Lim SR, Kim GS, Heo K, Park SC, Chang JW, Chung SS, Choi JU, Kim TS, Lee BI. Ictal electrocorticographic findings related with surgical outcomes in nonlesional neocortical epilepsy. Epilepsy Res. 2002; 48:199–206. [PubMed: 11904238]

Prince DA. Neurophysiology of epilepsy. Annu. Rev. Neurosci. 1978; 1:395–415. [PubMed: 386906]

Pulsinelli WA, Brierley JB, Plum F. Temporal profile of neuronal damage in a model of transient forebrain ischemia. Ann. Neurol. 1982; 11:491–498. [PubMed: 7103425]

Racine RJ. Modification of seizure activity by electrical stimulation. II. Motor seizure. Electroencephalogr. Clin. Neurophysiol. 1972; 32:281–294. [PubMed: 4110397]

Ramakers GJ, Corner MA, Habets AM. Development in the absence of spontaneous bioelectric activity results in increased stereotyped burst firing in cultures of dissociated cerebral cortex. Exp. Brain Res. 1990; 79:157–166. [PubMed: 2311692]

Richards DA, Morrone LA, Bagetta G, Bowery NG. Effects of alpha-dendrotoxin and dendrotoxin K on extracellular excitatory amino acids and on electroencephalograph spectral power in the hippocampus of anaesthetised rats. Neurosci. Lett. 2000; 293:183–186. [PubMed: 11036191]

Sakatani S, Seto-Ohshima A, Shinohara Y, Yamamoto Y, Yamamoto H, Itohara S, Hirase H. Neural-activity-dependent release of S100B from astrocytes enhances kainate-induced gamma oscillations in vivo. J. Neurosci. 2008; 28:10928–10936. [PubMed: 18945900]

Salt TE. Mediation of thalamic sensory input by both NMDA receptors and non-NMDA receptors. Nature. 1986; 322:263–265. [PubMed: 2874492]

NIH-PA Author Manuscript

NIH-PA Author Manuscript

NIH-PA Author Manuscript

Schauwecker PE, Steward O. Genetic determinants of susceptibility to excitotoxic cell death: implications for gene targeting approaches. Proc. Natl. Acad. Sci. U.S.A. 1997; 94:4103–4108. [PubMed: 9108112]

Schmued LC, Hopkins KJ. Fluoro-Jade B: a high affinity fluorescent marker for the localization of neuronal degeneration. Brain Res. 2000; 874:123–130. [PubMed: 10960596]

Schwob JE, Fuller T, Price JL, Olney JW. Widespread patterns of neuronal damage following systemic or intracerebral injections of kainic acid: a histological study. Neuroscience. 1980; 5:991–1014. [PubMed: 7402461]

Shimada H, Uta D, Nabekura J, Yoshimura M. Involvement of Kv channel subtypes on GABA release in mechanically dissociated neurons from the rat substantia nigra. Brain Res. 2007; 1141:74–83. [PubMed: 17300765]

Silveira R, Siciliano J, Abo V, Viera L, Dajas F. Intrastriatal dendrotoxin injection: behavioral and neurochemical effects. Toxicon. 1988; 26:1009–1015. [PubMed: 3245048]

Simpson MT, MacLaurin JG, Xu D, Ferguson KL, Vanderluit JL, Davoli MA, Roy S, Nicholson DW, Robertson GS, Park DS, Slack RS. Caspase 3 deficiency rescues peripheral nervous system defect in retinoblastoma nullizygous mice. J. Neurosci. 2001; 21:7089–7098. [PubMed: 11549719]

Singer W, Gray CM. Visual feature integration and the temporal correlation hypothesis. Annu. Rev. Neurosci. 1995; 18:555–586. [PubMed: 7605074]

Sperk G. Kainic acid seizures in the rat. Prog. Neurobiol. 1994; 42:1–32. [PubMed: 7480784]

Trasande CA, Ramirez JM. Activity deprivation leads to seizures in hippocampal slice cultures: is epilepsy the consequence of homeostatic plasticity? J. Clin. Neurophysiol. 2007; 24:154–164. [PubMed: 17414971]

Traub RD, Wong K. Cellular mechanism of neuronal synchronization in epilepsy. Science. 1982; 216:745–747. [PubMed: 7079735]

Traub RD, Miles R, Wong RKS. Model of the origin of rhythmic population oscillations in the hippocampal slice. Science. 1989; 242:1319–1325. [PubMed: 2646715]

Traub, RD.; Jefferys, JGR.; Whittington, M. Fast oscillations in cortical circuits. MIT press; Cambridge, MA: 1999.

Uhlhaas PJ, Singer W. Neural synchrony in brain disorders: relevance for cognitive dysfunctions and pathophysiology. Neuron. 2006; 52:155–168. [PubMed: 17015233]

Weller U, Bernhardt U, Siemen D, Dreyer F, Vogel W, Habermann E. Electrophysiological and neurobiochemical evidence for the blockade of a potassium channel by dendrotoxin. Naunyn. Schmiedebergs. Arch. Pharmacol. 1985; 330:77–83. [PubMed: 2413375]

Whittington MA, Traub RD, Jefferys JG. Synchronized oscillations in interneuron networks driven by metabotropic glutamate receptor activation. Nature. 1995; 373:612–615. [PubMed: 7854418]

Wilson MA, McNaughton BL. Dynamics of the hippocampal ensemble code for space. Science. 1993; 261:1055–1058. [PubMed: 8351520]

Worrell GA, Parish L, Cranstoun SD, Jonas R, Baltuch G, Litt B. High-frequency oscillations and seizure generation in neocortical epilepsy. Brain. 2004; 127:1496–506. [PubMed: 15155522]

Ylinen AM, Miettinen R, Pitkänen A, Gulyas AI, Freund TF, Riekkinen PJ. Enhanced GABAergic inhibition preserves hippocampal structure and function in a model of epilepsy. Proc. Natl. Acad. Sci. U.S.A. 1991; 88:7650–7653. [PubMed: 1652757]

Zhang WQ, Rogers BC, Tandon P, Hudson PM, Sobotka TJ, Hong JS, Tilson HA. Systemic administration of kainic acid increases GABA levels in perfusate from the hippocampus of rats in vivo. Neurotoxicology. 1990; 11:593–600. [PubMed: 2087285]

Zhao M, Adams JP, Dudek SM. Pattern-dependent role of NMDA receptors in action potential generation: consequences on extracellular signal-regulated kinase activation. J. Neurosci. 2005; 25:7032–7039. [PubMed: 16049179]

NIH-PA Author Manuscript
NIH-PA Author Manuscript
NIH-PA Author Manuscript

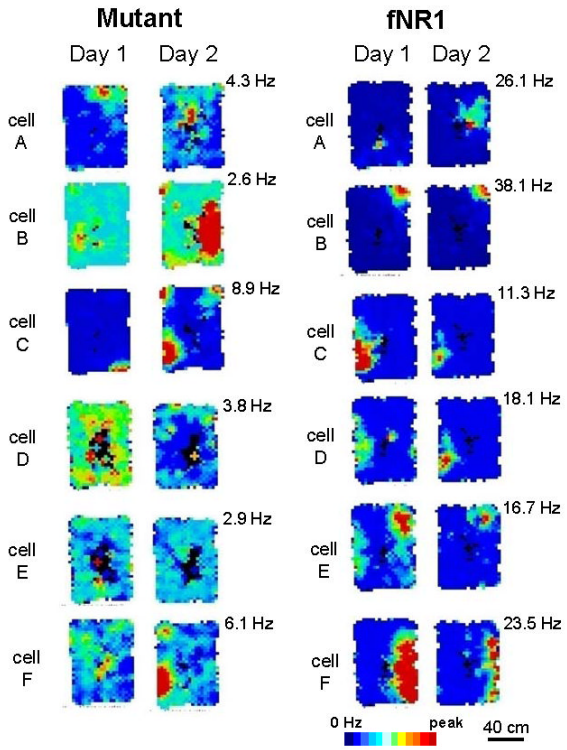

FIG. 1. Mutants are impaired in CA3 place cell activity in a novel and familiar arena

Representative place fields from the same CA3 complex spiking cells recorded in a novel (Day 1) and familiar (Day 2) rectangular low-walled arena (90 × 60 cm). Firing-rate maps are scaled to the same maximum firing rate per cell across days, as indicated at the upper right corner of the maps. Analysis was restricted to periods when animals were running >2 cm/sec and firing rate was calculated for pixels visited >10 times. The mutant mice displayed defective CA3 place cell activity, while CA3 cells in fNR1 control mice formed stable and spatially confined place fields.

NIH-PA Author Manuscript
NIH-PA Author Manuscript
NIH-PA Author Manuscript

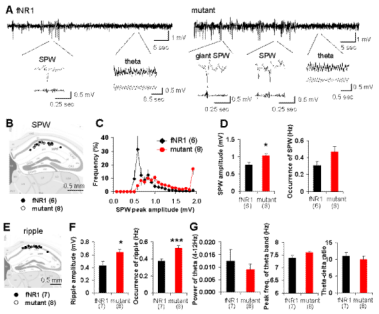

FIG. 2. Augmented SPW-R activity and normal theta wave activity in area CA1 of the mutants

(**A**) Representative LFP traces including theta and SPW-associated periods in fNR1 (left) and mutant (right) mice recorded from CA1 stratum radiatum. Typical traces of theta waves, 'conventional' SPWs and 'giant SPWs' are magnified below. LFP signals were filtered at 80-250 Hz to detect ripples and at 5-12 Hz to detect theta waves.

(**B**) Location of individual electrodes implanted in CA1 stratum radiatum for SPW analysis.

(**C**) Distribution of the peak amplitude of SPW in fNR1 control (black rhomboid) and mutant (red circle) mice. Strikingly, mutants showed clear bimodal distribution of SPW peak amplitude. Events with peak amplitude exceeding 1.8 mV were defined as 'giant SPW', which appeared only in mutants.

(**D**) The amplitude (left) and the occurrence (right) of conventional SPW in fNR1 and mutant mice during SPW-associated periods. Mutants displayed higher amplitudes (Student's *t*-test, **P*<0.05) and increased tendency towards 'conventional' SPWs (Student's *t*-test, *P*=0.09).

(**E**) Location of individual electrodes implanted in CA1 stratum pyramidale for ripple analysis.

(**F**) The amplitude (left) and the occurrence (right) of ripples in fNR1 and mutant mice during SPW-associated period. Ripple amplitude and occurrence in mutant mice were higher than in fNR1 controls. Student's *t*-test, ****P*<0.005, **P*<0.05.

(**G**) Power (left) and peak frequency (middle) of theta oscillations and theta-delta ratio (right) are shown. Theta/delta ratio was defined as power in the theta peak frequency range (5-10 Hz) divided by power in the delta peak frequency range (2-4 Hz). No significant differences in theta properties were observed between fNR1 and mutant mice, suggesting normal theta activity in mutants. Black bar, control mice; red bar, mutant mice. Number in parentheses indicates the number of animals.

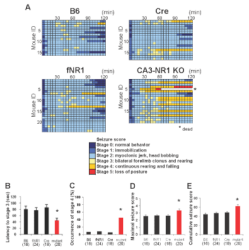

FIG. 3. CA3-NR1 KO mice show higher susceptibility to KA-induced seizures

(**A**) Time course of seizure severity in each animal from the mutant and three control genotypes (B6, fNR1 and Cre) following KA treatment (20 mg/kg, i.p.). The maximum seizure score of each animal was measured every 5 min over a 2-h period. Timescale in one box was 5 min.

(**B**) The latency to ‘stage 3′ seizures—forelimb clonus and rearing—was shorter in mutants than other genotypes. Note that, if the animal did not show stage 3 seizure, the latency was regarded as 120 min. Kruskal-Wallis test, **P*<0.05.

(**C**) The occurrence of ‘stage 4′ seizures—continuous rearing and falling—was higher in mutants than other genotypes. Fisher’s exact test, **P*<0.05.

(**D** and **E**) Mutant mice showed a higher severity of seizure than any of the control genotypes. Columns represent the averaged maximum seizure score (**D**) and cumulative seizure score (**E**) measured over a 2-h period after KA injection. Kruskal-Wallis test, **P*<0.05. Black bar, fNR1 mice; red bar, mutant mice. The number in parentheses indicates the number of animals.

NIH-PA Author Manuscript NIH-PA Author Manuscript NIH-PA Author Manuscript

NIH-PA Author Manuscript
NIH-PA Author Manuscript
NIH-PA Author Manuscript

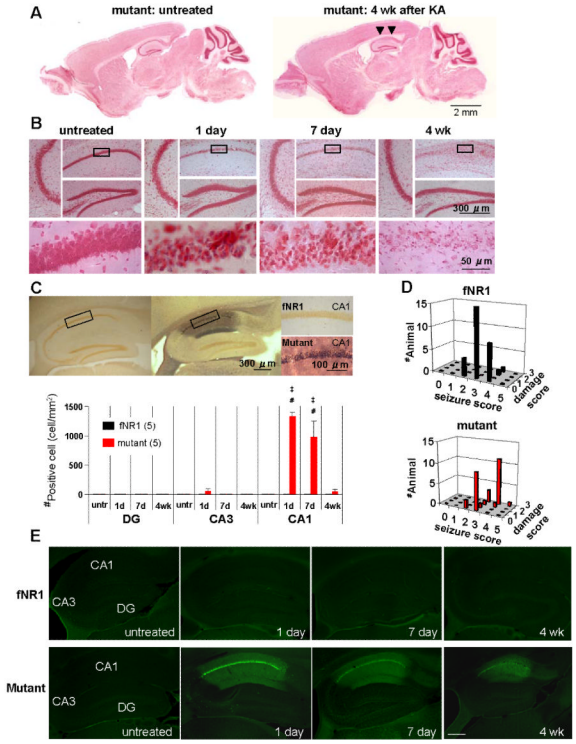

FIG. 4. KA-treated mutant mice showed massive neurodegeneration in area CA1

(**A**) Nissl-stained parasagittal brain sections of mutant untreated (left) and mutant 4 wk after KA treatment (right). KA-treated mutants showed severe neuronal loss in area CA1 (indicated by arrowheads).

(**B**) Magnified hippocampal subfields, CA1, CA3 and dentate gyrus (DG) in mutant mice untreated, or 1 day, 7 days and 4 wk after KA injection. Each bottom panel shows a higher magnification of the boxed area in the mutant CA1. Note that highly condensed pyknotic nuclei, a typical sign of damaged nuclei, were observed in the mutant CA1 pyramidal cell layer from 1 day to 7 days after KA injection, eventually disappearing by 4 wk post-treatment.

(**C**) Neurosilver staining showed massive neuronal degeneration in mutant CA1 7 days after KA treatment. Neurosilver-positive cells were not detected in the fNR1 control hippocampus. The graph on the right shows the number of neurosilver-positive cells in the hippocampal subfields of both genotypes. The number of neurosilver-positive cells in the mutant CA1 was significantly higher than in controls at 1-day or 7-day post-injection. Tukey's *post hoc* test, untreated mutant vs mutant at 1 day and 7 days after KA treatment, $^{\ddagger}P<0.0005$; fNR1 vs mutant at 1 day and 7 days after KA treatment, $^{\#}P<0.0005$. Black bar, fNR1 mice; red bar, mutant mice. The number in parentheses indicates the number of animals for each time point.

(**D**) 3D plots of maximum seizure scores (x axis) vs damage scores (y axis) of fNR1 (left) and mutant (right) mice 1 to 4 wk after KA treatment. Z axis shows number of animals. Neuronal damage was evaluated according to the damage score scale (see Methods). Black bar, fNR1 mice; red bar, mutant mice.

(**E**) Fluoro-Jade B staining revealed massive neuronal degeneration predominantly in the CA1 of the mutant mice 1 day, 7 days, and 4 wk after KA treatment, while almost no staining was observed in fNR1 controls and in untreated mouse sections regardless of genotype.

NIH-PA Author Manuscript
NIH-PA Author Manuscript
NIH-PA Author Manuscript

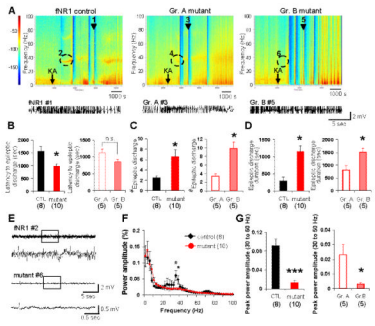

FIG. 5. Increased epileptic discharges with diminished gamma oscillation upon KA injection

(**A**) Representative spectrograms of KA-induced LFP activity from fNR1 control (left) and mutants (middle and right). Mutants were subdivided into two groups; Group A (middle), which did not show cell death, and Group B (right), in which CA1 cell death was eventually observed, based on the CA1 damage score shown in the middle panel of Fig. 9A. Arrows indicate timing of KA i.p. injection. Color: Log of power spectral densities. Epileptic discharge traces of a representative fNR1 mouse (marked as #1 in spectrogram) and Group A and Group B mutant mice (marked as #3 and #5, respectively) are also shown below each spectrogram.

(**B**) Left: the latency to epileptic discharges after KA treatment was shorter in mutant mice (n=10) than controls (n=8, 5 fNR1 and 3 Cre mice). Right: Group A 'non-cell death' mutants (n=5) and Group B 'cell death' mutants (n=5), as defined above. Student's *t*-test, **P*<0.05. No difference in latency to epileptic discharge was noted between the two mutant groups. Student's *t*-test, n.s., not significant.

(**C**) Left: epileptic discharges during 90 min after KA treatment occurred in mutant mice (n=10) more frequently than controls (n=8, 5 fNR1 and 3 Cre mice). Right: the number of discharges was higher in Group B mutants than in Group A mutants. Student's *t*-test, **P*<0.05.

(**D**) Left: average duration of individual epileptic discharge events was longer in mutants compared to controls. Right: among mutants, Group B mutants showed longer epileptic discharge duration than Group A mutants. Student's *t*-test, **P*<0.05.

(**E**) Representative traces of 30-50 Hz gamma band oscillatory activity, which preceded the first epileptic discharge, in fNR1 (upper) and Group B mutant (bottom) mice (marked as #2 and #6, respectively in Fig. 5A). Boxed periods in each upper trace are magnified in bottom traces.

(**F**) LFP power spectra in area CA1. The power amplitude of 30-50 Hz gamma band during 2 min before the onset of the first epileptic discharge was significantly diminished in mutants (red-filled circle) compared to controls (filled rhomboid). Student's *t*-test, $^{\#}P$<0.01 for 35 Hz, **P*<0.05 for 37.5 Hz.

(**G**) Left: peak power amplitude of 30-50 Hz gamma band oscillation in mutants was significantly attenuated compared to controls. Right: this attenuation was more prominent in Group B mutants compared to Group A mutants. Student's *t*-test, ****P*<0.00005, **P*<0.05. Black bar, fNR1 control mice; red bar, mutant mice; open red bar, Group A mutant mice; pink-filled bar, Group B mutant mice. The number in parentheses indicates the number of animals.

NIH-PA Author Manuscript

NIH-PA Author Manuscript

NIH-PA Author Manuscript

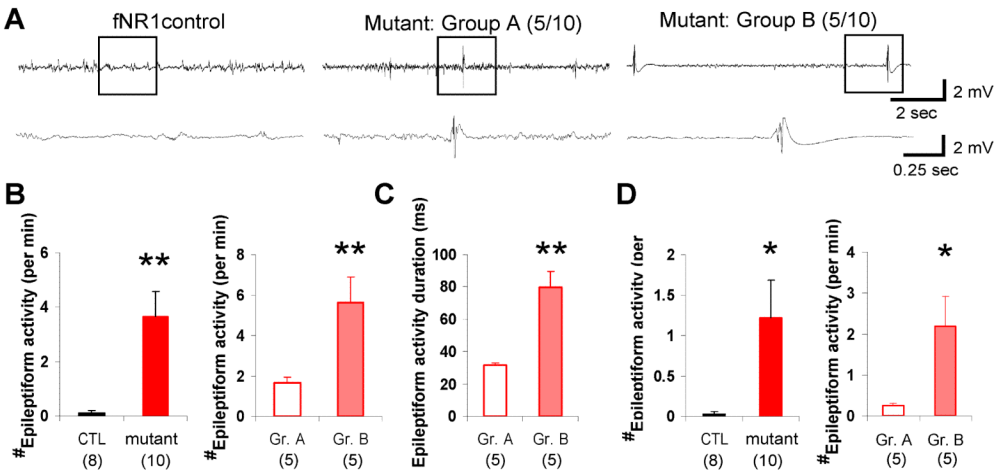

FIG. 6. Sustained epileptiform activity leading to cell death in area CA1 of mutant mice

(**A**) Representative LFP activity traces recorded 1 day after KA in fNR1 controls (left), Group A 'non-cell death' mutants (middle) and Group B 'cell death' mutants (right). Boxed periods in each upper trace are magnified in bottom trace. Epileptiform activity was present in mutants 1 day after treatment; controls showed almost normal activity. Group A mutants sporadically showed spike and wave discharges with concomitant background activity whereas Group B mutants displayed a burst suppression-like pattern.

(**B**) Group B mutants showed higher occurrence of epileptiform activity than Group A mutants (right). Almost no activity was observed in control mice (left). Mann-Whitney *U*-test, ***P*<0.005.

(**C**) Group B mutants showed longer duration of brief epileptiform activity events than Group A mutants. Student's *t*-test, ***P*<0.005.

(**D**) Burst-like epileptiform activities were still detected in Group B mutants 7 days after KA treatment (right), but were rarely observed in Group A mutants or control mice (left). Mann-Whitney *U*-test, **P*<0.05. Black bar, fNR1 mice; red bar, mutant mice; open red bar, Group A mutant mice; pink bar, Group B mutant mice. The number in parentheses indicates the number of animals.

NIH-PA Author Manuscript
NIH-PA Author Manuscript
NIH-PA Author Manuscript

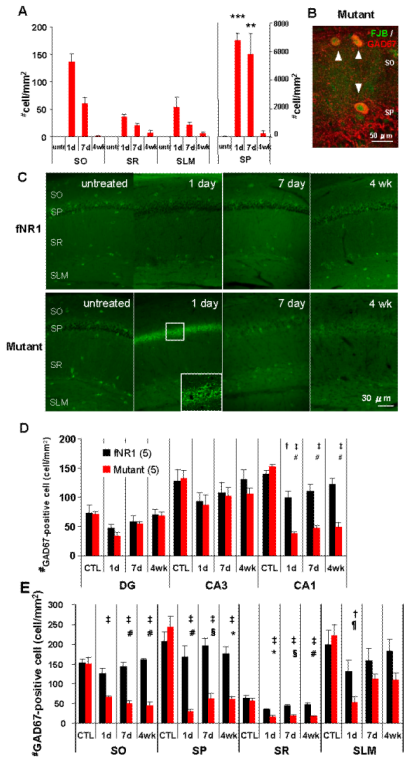

FIG. 7. Massive neurodegeneration of mutant CA1 interneurons after KA treatment

(**A**) Quantification of neurosilver-positive cell number in the mutant CA1 subfield in neurosilver-stained sections in Fig. 4C. One day after KA treatment, neurosilver-positive cells were significantly increased in the entire subfield. $F_{(3,16)}$=94.2 for SO, P<0.00001; $F_{(3,16)}$=21.8 for SP, P<0.0001; $F_{(3,16)}$=13.0 for SR, P<0.0005; $F_{(3,16)}$=5.84 for SLM, P<0.01, Tukey's *post hoc* test, untreated mutant vs mutant at each time point after KA treatment, ***P<0.0005, **P<0.001, *P<0.05.

(**B**) Confocal double staining image of Fluoro-Jade B (FJB, green) with GAD67-IR (red) 1 day after KA treatment, showing the degenerating GABAergic neurons in area CA1.

(**C**) Differential changes in GAD67-IR in area CA1 of fNR1 and the mutant mice 1 day, 7 days and 4 wk after KA treatment compared to their untreated CA1. Inset shows a confocal higher magnification of the boxed area in CA1, indicating the elevated GAD67-IR presumably localized to GABAergic neuron axon terminals. In mutant mice, GAD67-IR in the CA1 cell layer was paradoxically augmented 1 day after treatment (inset), suggesting massive GABA release, which was not observed in control mice.

(**D**) Quantification of GAD67-positive cells in the hippocampal subfields for each genotype. The number of GAD67-positive cells in the mutant CA1 was significantly lower in the fNR1 CA1 1 day, 7 days, and 4 wk after KA treatment; no differences were observed in CA3 or DG. $F_{(3,32)}$= 12.2 for genotype × time interaction in CA1, P<0.00005, Tukey's *post hoc* test, $^{\dagger}P$<0.05 for untreated fNR1 vs fNR1 1 day after KA treatment, $^{\ddagger}P$<0.0005 for untreated mutant vs mutant at each time point after KA treatment, $^{\#}P$<0.0005 for fNR1 vs mutant at each time point.

(**E**) Quantification of GAD67-positive cells inside the CA1 subfield for each genotype. Mutant GAD67-positive cells were severely and permanently decreased in the entire subfield except SLM, compared to the fNR1 control mice. $F_{(3,32)}$=10.7 for genotype × time interaction in SO, P<0.00005; $F_{(3,32)}$=8.60 for genotype × time interaction in SP, P<0.0005; $F_{(3,32)}$=3.24 for genotype × time interaction in SR, P<0.05; $F_{(3,32)}$=1.56 for genotype × time

NIH-PA Author Manuscript

NIH-PA Author Manuscript

NIH-PA Author Manuscript

interaction in SLM, P=0.21. Tukey's *post hoc* test, untreated mutant vs mutant at each time point after KA treatment, $^{\dagger}P<0.05$, $^{\ddagger}P<0.0005$; fNR1 vs mutant at each time point, $^{\P}P<0.05$, $^{*}P<0.01$, $^{\S}P<0.005$, $^{\#}P<0.0005$. Black bar, fNR1 mice; red bar, mutant mice. The number in parentheses indicates the number of animals for each time point. Stratum oriens (SO), stratum pyramidale (SP), stratum radiatum (SR), and stratum lacunosum-moleculare (SLM).

NIH-PA Author Manuscript
NIH-PA Author Manuscript
NIH-PA Author Manuscript

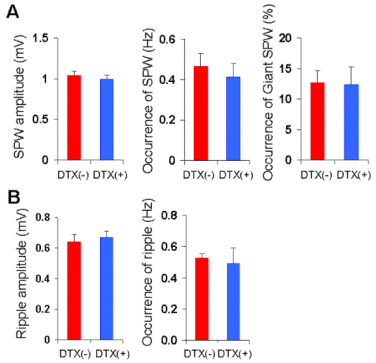

FIG. 8. DTX treatment did not affect mutant SPW-R complex activity

(**A**) The amplitude (left) and occurrence (middle) of conventional SPW, and the occurrence (relative value) of 'giant SPW' (right) in mutants before (red) and after (blue) DTX treatment (n=9). (**B**) The amplitude (left) and the occurrence (right) of mutant ripples before (red) and after (blue) DTX treatment (n=9). No significant change in SPW-R activity was observed before and after DTX treatment (Student's *t*-test, P=0.09, P=0.61, P=0.88, P=0.68 P=0.73 for SPW amplitude, SPW occurrence, the ratio of giant SPW, ripple amplitude, and ripple occurrence, respectively). The number in parentheses indicates the number of animals.

NIH-PA Author Manuscript
NIH-PA Author Manuscript
NIH-PA Author Manuscript

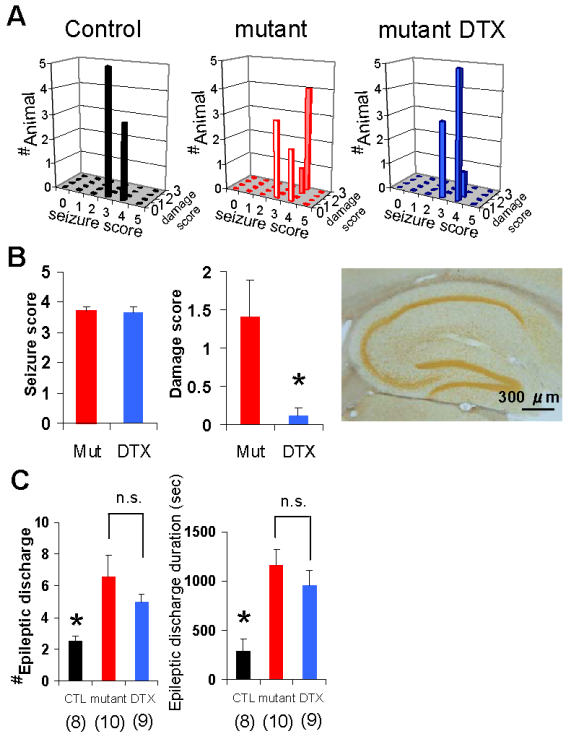

FIG. 9. Pretreatment with DTX protected CA1 cells from neurodegeneration but failed to attenuate the severity of epileptic discharges in mutant mice

(**A**) 3D plots of the maximum behavioral seizure scores (x axis) vs the CA1 damage scores (y axis) of fNR1 (left, n=8), mutant (middle, n=10) and DTX-pretreated mutant (right, n=9) mice during 90 min after KA treatment. Z axis shows the number of individual mice. A subconvulsive dose (0.5 mg/kg) of DTX prevented mutants from KA-induced massive CA1 cell damage. Behavioral seizure severity induced by KA was not affected by DTX.

(**B**) Quantification of CA1 damage score (middle) in mutant with or without DTX pretreatment suggests DTX prevented KA-induced excitotoxicity (Student's *t*-test, **P*<0.05). No difference was observed in behavioral seizure scores between the genotypes (left). Right: representative photomicrograph of Neurosilver staining in CA1 from DTX-pretreated mutants 1 wk after KA treatment, showing no cell death in CA1.

(**C**) The number (left) and duration (right) of mutant epileptic discharge during 90 min after KA injection was not affected by DTX pretreatment. DTX-pretreated mutants had a higher number of epileptic discharges and their longer duration than control mice, but there were no differences for both measures between DTX-pretreated mutants and mutants without DTX. Discharge number, Kruskal Wallis test, $P<0.005$, Mann-Whitney *U*-test with Bonferroni correction for multiple comparisons, $P<0.05$ for controls vs DTX--pretreated mutants, $P=1.0$ for mutants vs DTX-pretreated mutants; Discharge duration; $F_{(2, 24)}=8.86$, $P<0.005$, Bonferroni *post hoc* test, $P<0.05$ for controls vs DTX-pretreated mutants, $P=1.0$ for mutants vs DTX-treated mutants. The number in parentheses indicates the number of animals.

NIH-PA Author Manuscript

NIH-PA Author Manuscript

NIH-PA Author Manuscript

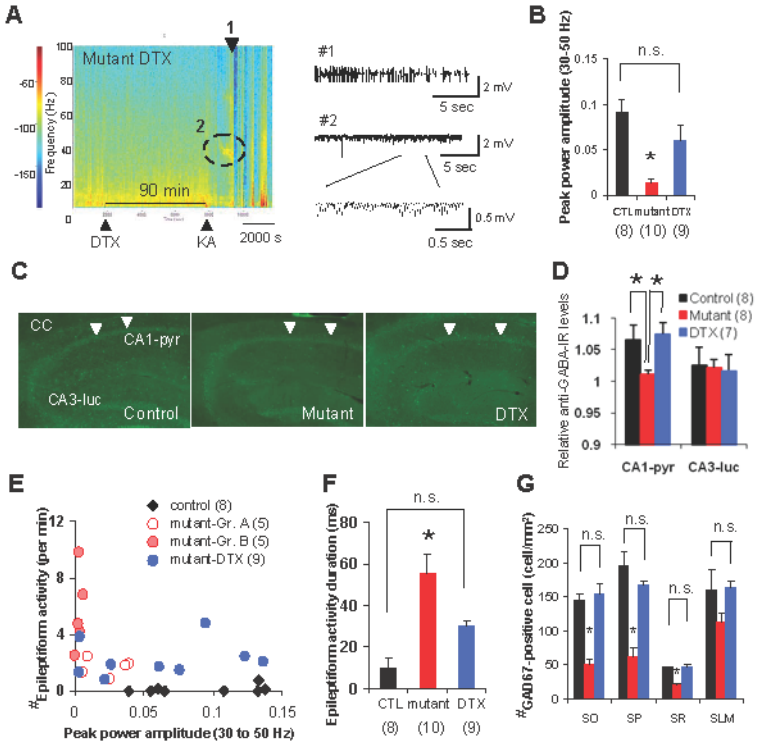

FIG. 10. Pretreatment with DTX restored gamma oscillation and GAD67 activity and diminished epileptiform activity and CA1 degeneration

(**A**) Left: a representative spectrogram of KA-induced LFP activity in DTX-pretreated mutants. DTX injection occurred 90 min before KA injection. Color: log of power spectral densities. Right: epileptic discharge trace (marked as #1) and a representative trace of 30-50 Hz gamma band oscillatory activity (marked as #2) of DTX-pretreated mutants.

(**B**) Peak power amplitude of 30-50 Hz gamma band oscillations in the DTX-pretreated mutants was significantly higher than in mutants without DTX, and was the same level as control mice, suggesting restored low frequency gamma oscillations by DTX-pretreatment. $F_{(2,24)}$=9.98, P<0.001, Bonferroni *post hoc* test, P=0.32 for controls vs DTX-pretreated mutants, *P<0.05 for mutants vs DTX-treated mutants.

(**C**) The representative photomicrographs for GABA-IR of controls (left), mutants (middle), and mutants with DTX-pretreatment (DTX, right) 20 min after KA treatment. Arrowheads indicate CA1 cell layers.

(**D**) An increase in GABA level was observed in CA1 pyramidal cell layer (CA1-pyr) but not in stratum lucidum in CA3 (CA3-luc) in control animals 20 min after systemic KA i.p. injection. This KA-induced GABA release was abolished in the mutants, but restored after pretreatment with DTX. This mutant deficit was observed in the CA1 cell layer, but not in area CA3. Images were obtained by confocal microscope using ×10 objective. The relative GABA-IR values were normalized to the level of corpus callosum-IR. Kruskal-Wallis test followed by *post-hoc* Mann-Whitney test with Bonferroni's correction, *P<0.05.

(**E**) Scatter plot of the peak power amplitude of gamma oscillations vs the number of epileptiform activity 1 day after KA treatment of fNR1 (filled rhomboid), mutants (open red circle for Group A mutants, pink circle for Group B mutants) and DTX-pretreated mutants (blue circle). Each dot represents an individual mouse. DTX diminished the epileptiform activity and restored low frequency gamma oscillations.

(**F**) The duration of the mutant epileptiform activity 1 day after KA treatment was dramatically decreased by DTX pretreatment. $F_{(2,24)}$=11.7, P<0.0005 for genotype effect,

NIH-PA Author Manuscript

NIH-PA Author Manuscript

NIH-PA Author Manuscript

Bonferroni *post hoc* test, P=0.15 for control vs DTX-pretreated mutants, *P<0.05 for mutant vs DTX-pretreated mutants.

(**G**) Representative photomicrograph of GAD67-IR in DTX-pretreated mutants 1 wk after KA treatment. Quantitative analysis of GAD67-positive cell in the CA1 subfield showed no differences between control mice and DTX-pretreated mutants, suggesting DTX pretreatment fully preserved GABAergic function in the mutant CA1. Black bar, fNR1 mice; red bar, mutant mice. Open red bar, Group A mutant mice; pink bar, Group B mutant mice. $F_{(2,13)}$=24.21 for SO, P<0.00005, Bonferroni *post hoc* test, P=1.0 for controls vs DTX-pretreated mutants, *P<0.0001 for mutants vs DTX-treated mutants; $F_{(2,13)}$=25.9 for SP, P<0.00005, Bonferroni *post hoc* test, P=0.44 for controls vs DTX-pretreated mutants, *P<0.00005 for mutants vs DTX-treated mutants; $F_{(2,13)}$=20.6 for SR, P<0.0001, Bonferroni *post hoc* test, P=1.0 for controls vs DTX-pretreated mutants, *P<0.0005 for mutants vs DTX-treated mutants; $F_{(2,13)}$=2.17 for SLM, P=15, Bonferroni *post hoc* test, P=1.0 for controls vs DTX-pretreated mutants. Stratum oriens (SO), stratum pyramidale (SP), stratum radiatum (SR), and stratum lacunosum-moleculare (SLM). The number in parentheses indicates the number of animals. n.s., not significant.

NIH-PA Author Manuscript

NIH-PA Author Manuscript

NIH-PA Author Manuscript

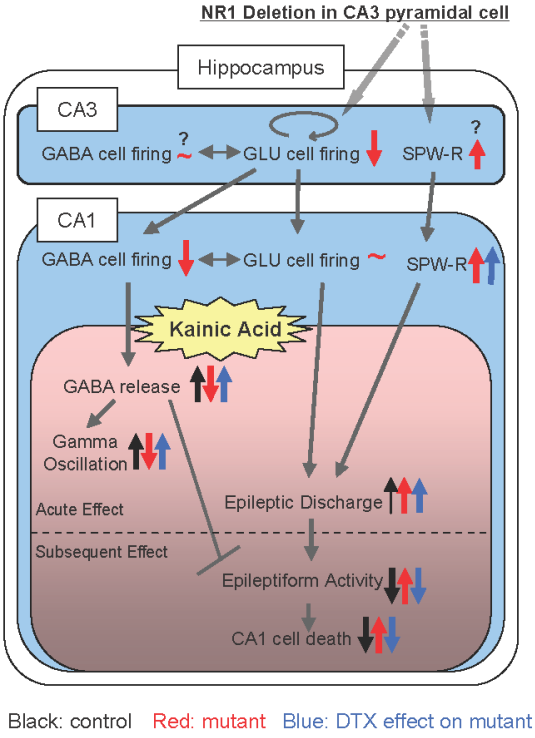

FIG. 11. KA-induced gamma oscillations and CA1 cell death in CA3-NR1 KO mice

Depiction of how genetic deletion of CA3-NR1 influences CA3-CA1 network activity (blue) and, upon KA administration, undergoes CA1 neurodegeneration (pink). Post-adolescent NR1 elimination in CA3 pyramidal cells (GLU cells) diminishes their action potential firing, thereby reducing the firing of CA1 interneurons (GABA cell) while CA1 pyramidal cell activity is maintained by reduced feed-forward inhibition. Simultaneously, CA3-NR1 deletion abnormally enhances sharp wave-ripple (SPW-R) activity in CA3. An intermediate dose of kainic acid (KA, 20 mg/kg, i.p.) facilitates GABA release, thereby eliciting 30-50 Hz gamma oscillations within 20 min, then evoking epileptic discharge-burst activity in the control animals (black arrow). However, this dose does not extend the epileptic discharges to the sustained epileptiform activity on the following days, and consequently, no cell death is observed in the control hippocampus. In contrast, KA-induced GABA release and gamma oscillations do not occur in area CA1 of the mutants, presumably due to reduced excitability of CA1 interneurons, and epileptic discharges are instead exacerbated, along with an enhancement of SPW-R activity (red arrow). A presynaptic GABA release enhancer, DTX (blue arrow), has no effect on mutant SPW-R activity and seizure severity after KA administration. Remarkably, however, it assists in KA-induced GABA release which maintains the integrity of the CA1 GABAergic network, thereby preserving gamma oscillations, suppressing epileptiform activity, and further protecting mutant CA1 from KA-induced excitotoxicity. These results suggest that KA-induced GABA release may prevent epileptic discharges from transforming the sustained epileptiform activity and deteriorating GAD67-positive cells, which results in no neurodegeneration of CA1 neurons. Overall, the emergence of KA-induced gamma oscillations predicts good prognosis against KA-induced hippocampal excitotoxicity in mice. Question mark denotes putative action/change.

NIH-PA Author Manuscript

NIH-PA Author Manuscript

NIH-PA Author Manuscript

Table 1

Properties of CA3 pyramidal cells in familiar linear tracks

Measurement	fNR1	Mutant
Mean firing rate (Hz)	2.38 ± 0.36	0.55 ± 0.09**
Peak firing rate (Hz)	14.5 ± 2.09	7.46 ± 1.31*
Spike width (μS)	542.8 ± 19.4	574.6 ± 20.2
Burst duration (ms)	10.6 ± 0.3	8.9 ± 0.5*
Burst spike frequency (%)	41.9 ± 2.2	33.4 ± 2.5*

20 neurons from 3 fNR1 controls and 25 neurons from 4 mutants. Student's t-test

* $P<0.05$

** $P<0.0005$